CAD ASSISTED DEVELOPMENT OF DUAL BAND OSCILLATOR AND ITS INTEGRATION WITH RADIATING ELEMENTS

A DISSERTATION

Submitted in partial fulfillment of the
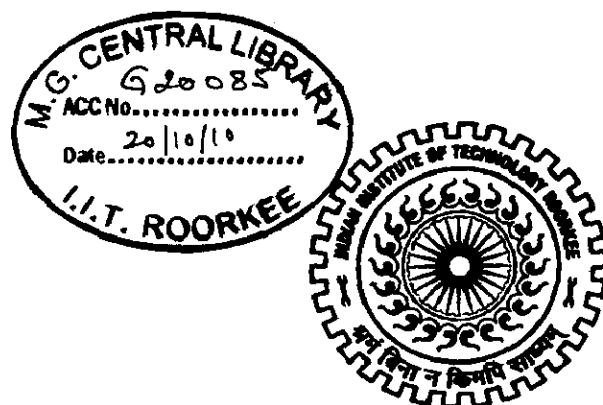*requirements for the award of the degree*
of
MASTER OF TECHNOLOGY
in
ELECTRONICS AND COMMUNICATION ENGINEERING
(With Specialization in RF & Microwave Engineering)

By
RAVINDER YADAV

DEPARTMENT OF ELECTRONICS AND COMPUTER ENGINEERING
INDIAN INSTITUTE OF TECHNOLOGY ROORKEE
ROORKEE -247 667 (INDIA)
JUNE, 2010

Candidate's Declaration

I hereby declare that the work, which is being presented in the dissertation entitled, *"CAD Assisted Development of Dual Band Oscillator and its Integration with Radiating Elements"*, which is submitted in the partial fulfillment of the requirements for the award of degree of *Master of Technology* in *RF & Microwave Engineering*, submitted in the Department of Electronics and Computer Engineering, *Indian Institute of Technology*, Roorkee (INDIA), is an authentic record of my own work carried out under the supervision of **Dr. N.P. Pathak**, Assistant Professor, Department of Electronics and Computer Engineering, Indian Institute of Technology, Roorkee.

I have not submitted the matter embodied in this dissertation for the award of any other degree or diploma.

Date: June 28, 2010

Place: Roorkee
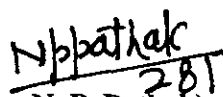
(Ravinder Yadav)

Enroll. No: 08533010

Supervisor's Certificate

This is to certify that this dissertation entitled, *"CAD Assisted Development of Dual Band Oscillator and its Integration with Radiating Elements"*, which has been submitted by Ravinder Yadav is record of his own work carried out by him under my supervision. I also certify that the above statement made by the candidates is correct to the best of my knowledge and belief.

Date: June 28, 2010
Place: Roorkee

(Dr. N. P. Pathak)
Assistant Professor
E&CE Department
IIT – Roorkee
Uttaranchal – 247667

[ii]

It has been a great privilege to be an M.Tech student in the Electrical and Computer Engineering department at IIT, Roorkee and work closely with my advisor **Dr. N. P. Pathak,** Assistant Professor, Department of Electronics and Computer Engineering, IIT Roorkee. His keen insight into system and integrated circuit design is the key factor in the success of this research. I express my deepest gratitude to him for his valuable guidance, support and motivation in my work. I have deep sense of admiration for his inexhaustible enthusiasm and readiness to help me. The valuable discussions and suggestions with him have helped me a lot in supplementing my thoughts in the right direction for attaining the desired objective.

Special thanks are due to **Prof. S. N. Sinha,** Head of the Department, Electronics and Computer Engineering, for providing the necessary facilities to carry out this dissertation work. I also thank him for his continuous support and expert comments.

I thank **Mr. Rajaram, Mr. SK Gaur and Mr. Giri** for their valuable support and time to time guidance in technical issues, which was instrumental in making this dissertation work a success. My special sincere heartfelt gratitude to all my friends, whose sincere prayer, best wishes, support and unflinching encouragement has been a constant source of strength to me during the entire work. Finally, I would like to thank my family for always being by my side and their support.

(Ravinder Yadav)

This dissertation reports the design and development of single HEMT based switched resonator dual-band oscillator for 5.2/6.8 GHz wireless applications. Fixed dual band operation was achieved by introducing a novel band switching technique for controlling the negative resistance bandwidth of the HEMT. Oscillator characteristics were optimized to meet the specified IEEE standards. Switched resonators based on membrane and semiconductor switch behavior were also investigated. Commercially available simulation tools ADS and EMDS were used in the modeling of this novel device.

Further, the integration of this oscillator with the planar radiating elements were also investigated. A microstrip patch antenna at 5.2 GHz was designed and used as frequency selective network in the oscillator circuitry. The simulated and measured characteristics of oscillator, integrated with radiating element were found to be as per the requirement of 802.11b and 802.11a ISM standards.

Table of Contents

Figures

Tables

Review of Literature

1.1 Introduction

Multi-band oscillators are expected to become key components in the next generation multi-band and multi-mode wireless radios [1]. Conventionally, a wireless device operates in a specific frequency band, as required for some specific application. However, since a user desire to make best use of the available wireless resources, devices providing multiple services simultaneously are required. This is because a single device, providing multiple functionalities, reduces the burden of carrying multiple devices. Furthermore, the advent of wireless systems as well as their evolution over the years has acted as catalysts in development and further enhancement of multi-band networks.

RFICs form a major part of the modern wireless communication systems [2] due to its ability to implement a number of functions in continuously shrinking integrated circuits. In general, an integrated circuit containing analog circuitry operating at and above ultra-high frequency (UHF) band is defined as a Radio Frequency Integrated Circuit (RFIC). The ICs can be classified into the MMIC (Monolithic Microwave Integrated Circuits) and Hybrid ICs (Hybrid Integrated Circuits) [3]. The oscillator type active integrated antenna has seen a growing interest in recent years, as the microwave integrated circuit (MIC) and monolithic microwave integrated circuit (MMIC) technologies have became more mature allowing for high-level integration. Hybrid ICs, which is a combination of distributed and lumped components are focused in the dissertation.

RF (radio frequency) and microwave oscillators are universally found in all modern radar and wireless communications systems to provide signal sources for frequency conversion and carrier generation [4]. An oscillator is very important part of any radio-frequency hardware, e.g., transceiver front-end as shown in Fig. 1.1. Microwave oscillator represents the basic microwave energy source for all microwave systems, such as radar communications, navigation, and electronic warfare. They can be termed as DC-to-RF converters or infinite gain amplifiers [5]. For dual-band operation, each of these individual blocks may be implemented to give a dual band performance or a part of the circuit can be designed to exhibit dual band operation.
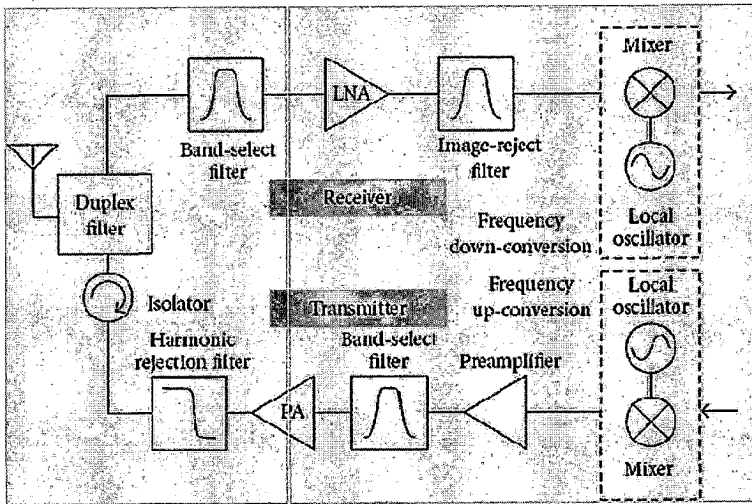
Fig. 1.1 Typical Transceiver Front-End [1]

The remaining components can be optimized to work on individual respective frequencies, so that a balance between space constraints and performance optimization can be achieved. There has been some progress in research for linear components like amplifiers for multi-band operation, whereas the non-linear components like oscillator are preferably designed for a single frequency operation [2-3]. Designing a non-linear circuit to operate at multiple frequencies can be quite complex and challenging. Nevertheless, there has not been much research on RFIC implementation of dual band oscillator using single transistor. In summary, the design of dual-band oscillator is an open field of research. Adding radiating element to these blocks creates more challenges in the design from circuit as well as system point of view and can prove to be a potentially valuable future research direction.

1.2   Literature Review

The recent migration and upsurge in the demand for portable wireless communication products for the 5-GHz WLAN (wireless local area network) applications has caused much

research interest in Oscillator type Active Integrated Antenna (AIA) technology, where the passive radiating element is integrated with an active device in the front-end of RF systems. In active devices, dual-band performance has been achieved in linear as well as the non-linear modes of operation [6-7]. Dual band architectures are becoming necessary to overcome possible interference from the saturation of the 5.2-GHz band, thus allowing data to be transmitted in both the 5.2- and 6.8-GHz bands. With the market pushing towards dual-band systems, the operating system must have higher levels of integration in order to reduce size, external component count, and cost of the devices on an integrated circuit [2].

Various architectures have been proposed for design and implementation of dual-band transceiver. The simplest approach is parallel architecture having different paths for each individual frequency. This makes circuit bulky and is equivalent to combining the components of different receivers on a single chip [8]. This architecture has the advantage of low interference and each stage can be optimized separately. However, owing to the large die area it occupies, the layout and PCB design becomes difficult. A modification to the parallel architecture can be achieved by having a switched network, selecting the path corresponding to the incoming RF frequency. The switch at the input of the circuit performs selection between the parallel paths for the incoming frequencies. In concurrent scheme, the same receiver architecture is designed in such a way so as to receive more than one frequency signals, simultaneously. Each stage is designed for operation in dual-band mode. However, design of such architecture is extremely challenging and an optimum gain cannot be achieved for all the bands. In other words, a compromise has to be made in the amount of gain achieved [9].

(A)   Oscillator Design:

Microwave oscillator consists of frequency selective circuit (resonator), negative resistance cell (transistor with positive feedback and biasing circuit) and output matching circuit [10] as shown in Fig. 1.2. There have been some methods that developed for the realization of a dual-band oscillator as discussed above, same concept can be used for dual-band oscillator i.e. two separate single-band oscillator in parallel, but it would result in an increase in the dissipation power, chip area and the module cost. Another way is to use switching approach for either frequency selective circuit or for output matching circuit with single transistor.
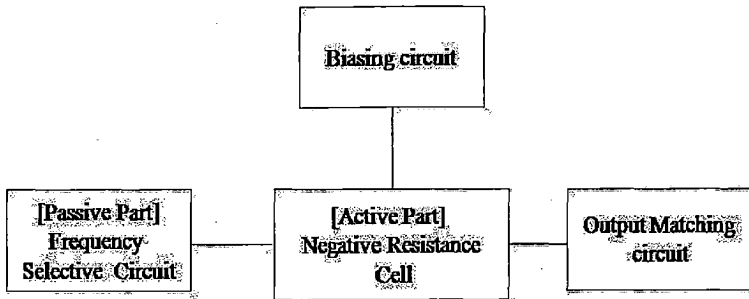
Fig. 1.2 Block diagram of negative resistance based typical oscillator

Majority of multi-band oscillators have switched oscillators, resonators or matching elements [11-15] to attain a dual-band performance. Efforts are being carried out to design a single matching network that matches the impedance at both the frequencies. This will reduce the circuit complexity and size. Dual-band matching networks using lumped components matches the transistor impedance to 50-Ohm at the two given frequencies and suppresses other frequencies.

There are two methods to switch the resonator frequency. One is a regenerative multiplication method, in which a frequency divider or a multiplier is used to obtain another band other than fundamental band [16] of a given VCO. The frequency band is determined by dividing or multiplying ratio. The other is a switched-capacitor method, which is more frequently used [15] at lower frequencies less than GHz. It employs a capacitor with a series connected switch, which controls the capacitance of a LC tank. In this case, the parasitic resistance of the switch degrades the quality factor of the LC tank. This becomes serious as operating frequency increases. As a consequence, phase noise performances get worse. While parasitic resistance decrease with larger switch, the parasitic capacitance of the switch also increases to reduce switching frequencies. This problem is taken care of by dual-band VCO structure, uses a balanced VCO core with buffer amplifiers, which oscillates both in differential mode as well as in common mode. The mode is selected by switching current sources. The dual-band VCO shows fast band-switching times of 20- and 4-ns between low to high and high to low band frequencies, respectively [17].

Another type of dual-band oscillators have been traditionally realized by reconfiguring the frequency selective network [18-19]. Typically, a cross-coupled negative resistance cell is combined with a switch-controlled resonator. Switched resonators are used to change the oscillation frequency either by connecting an inductor or a capacitor via a switch transistor to the main tank. However, because of limited channel resistance of the switch, the tank quality (Q) factor degrades up to 30%. Another technique involves the use of a transformer whose primary winding is connected to the main tank while the secondary winding is connected in parallel to a transistor [20]. The transistor acts as a switch or a voltage controlled resistor results varying the effective inductance seen in the primary winding. However this technique also suffers from the loss over the switch as a portion of the energy pumped into the tank is dissipated over the switch degrading the quality factor of the tank. The common feature of all prior techniques for multi-band oscillators is reconfiguring the resonator, which would consequently affect the tank quality factor. To overcome this difficulty a fixed high-order resonator was employed and the band switching mechanism was shifted from the tank to the loss compensation network (i.e., negative resistance network). This will maintain the high quality factor of the tank at multiple oscillation frequencies [21]. By moving the band switching mechanism to the active core of the oscillator, the overall performance can be simultaneously optimized for multiple frequency bands.

Most of work has been done for dual-band and multi-band oscillators with switched resonator using CMOS technology. In this regard, a 6/9-GHz dual band quadrature *LC*-tuned VCO based on the analog frequency multiplication method was implemented in a 0.18-μm SiGe BiCMOS technology. It can be reconfigured to generate output signals at either 6 or 9GHz depending through band selection [22].

(B)   Active integrated antennas (AIA)

Active integrated antennas (AIAs) have provided novel design technologies in modern RF/microwave system architectures for both military and commercial applications. Active integrated antennas have come into picture because of mature monolithic microwave-integrated circuit technology with antenna integration in a variety of transceiver applications, particularly at lower millimeter wave frequencies [23]. An active-integrated antenna, integrates the active microwave circuits and the radiating elements onto the same substrate, thereby, reducing transition and transmission losses.

Active-integrated antennas can be classified into three categories; oscillators, amplifiers, and frequency converters according to their functions. There is great interest in using an oscillator-type AIA for generating microwave and millimeter wave signals. AIA can be regarded as an active microwave circuit in which the output or input port is free space instead of a conventional 50-Ω interface. Herein, the antenna plays special roles such as resonating, filtering, and diplexing, as well as, a radiating element in a system circuitry.

The oscillator-type active-integrated antenna comprises of radiating element, feed and oscillator. To date, the microstrip patch antenna has been the most commonly used radiating element due to its lightweight, planar structure and ease of handling. There have been lots of efforts to design a compact oscillator with an antenna as unit elements of array systems for high power [24-25] and to design a frequency tunable oscillator with a controlled resonator. The oscillator type AIA converts dc power to RF power using negative resistance characteristics of an active device [26]. Proper selection of an operating point of the active device is important for the operational performance. An integrated version of such an active antenna has been developed for sensor applications at lower power levels.

An integrated antenna oscillator is formed by integrating an active solid-state device directly with an antenna. The active solid-state device could be a diode such as Gunn, IMPATT, BARITT, etc., or a transistor such as, MESFET, high electron-mobility transistor (HEMT), hetero-junction bipolar transistor (HBT), etc. In conventional approach, the antenna and the oscillator are two separate components interconnected by a transmission line. There is freedom to optimize the performance of the oscillator and the antenna, independently, because there is an obvious distinction between the circuit component and the radiating structure. In the integrated antenna oscillator, there is no obvious distinction or boundary between the oscillator and the antenna. The active device lies within the volume normally associated with the radiating structure. The antenna serves both as a load or frequency selective element and a radiator for the active device. An AIA oscillator has the advantages of smaller size, lower cost, and lower loss, as compared to the conventional approach.

Generally, FETs have higher efficiencies and lower noise figures than either IMPATT or Gunn diodes, and can be easily made monolithically. A microstrip patch antenna integrated with an FET transistor [27] is shown in Fig. 1.3. The circuit consists of a patch antenna, matching and bias circuitry. The oscillator is formed by placing a frequency

selective network, such as resonator, which is patch antenna, in the feedback loop of an amplifier. If the feedback is positive at the operating frequency, oscillation will occur. In this oscillator, the patch serves as both resonator for the FET oscillator circuit and a radiator.
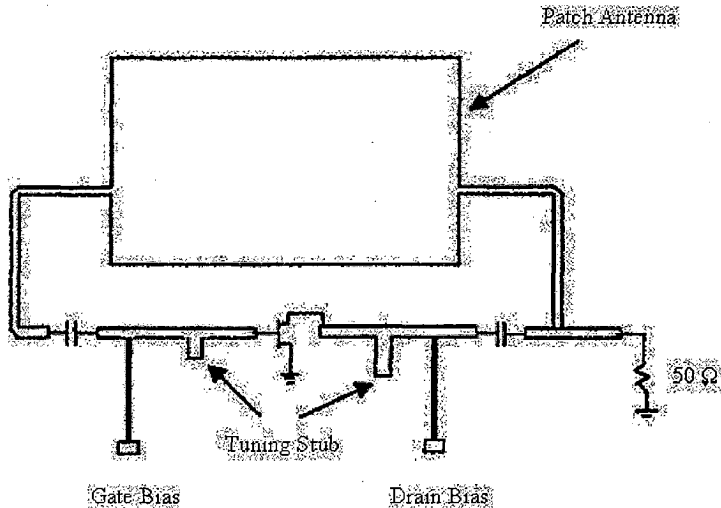
Fig. 1.3. Integrated FET patch antenna oscillator [27].

In the case of amplifier type active integrated antennas, two port active device is integrated with passive antenna element at input or output port for the purpose of signal amplification. When the antenna is at input port, it is considered to be source impedance for the device and the integrated antenna works as a receiver. The low noise amplifier design technique is usually applied in order to achieve the required noise performance.

When the antenna is placed at the output port, it acts as device load impedance. In this case, the integrated active antenna functions as a transmitter. An amplifier design technique for achieving gain bandwidth performance is generally applied [27]. FET location with respect to patch is shown in Fig. 1.4. when AIA operates as a transmitter and receiver respectively. The advantages of amplifier type active integrated antenna are gain and bandwidth enhancement and low noise performance.
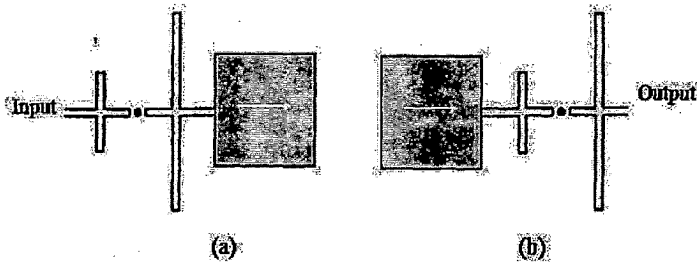
Fig.1.4. Amplifier type AIAs. (a). Transmitting type and (b). Receiving type.

1.3   Origin of the Problem

With the increase in demand and rapid improvements in the dual-band applications, the cost of wireless devices has considerably reduced. In this environment of decreasing cost and increasing complexity, acquiring more functionality and flexibility is the best objective for future integrated wireless devices. The dual frequency oscillator has been exploited by the researchers for making the dual band applications for various useful wireless communication bands. The advent of the wireless systems as well as their evolution over the years has acted as a catalyst to develop and then enhance dual-band oscillator.

Wireless local area network (WLAN) technology is a rapidly expanding area in the modern wireless communication and has received much attention for the flexibility of network reconfiguration in office room, mobile internet connection and so on. Single device can be used for two applications. To achieve more flexibility active integrated antenna with oscillator are used in different applications. Due to the enormous increase in the number of users and traffic many base stations are introduced each year mainly in highly populated areas. The use of dual-band oscillator allows a significant reduction in the number of oscillators providing an important improvement in terms of cost and size of the hardware.

Since, microstrip antennas have advantages of modest size, low profile, and planar geometry, leading to low manufacturing cost. The planar structure also lends itself to integration with the associated electronic circuits, e.g., in the form of an active antenna. Dual-band oscillator integrated with microstrip antennas is well suited for most of the wireless application systems. Miniaturization often requires integration of multiple components into

common, compact structures. One or more integration techniques can be used in conjunction to reduce the size of the system as per the requirement of the application. These needs and application-specific requirements have provided basic motivation to take up this specific problem to carry out my dissertation work. The present work is reported to meet the requirements of all applications including transceivers and WLAN (5.2/6.8 GHz) wireless applications. The dual-band oscillator will oscillate at 5.2GHz and 6.8GHz frequencies. These frequencies are available to use in the unlicensed industrial, scientific, and medical (ISM) bands allocated by the FCC, which is also in the IEEE 802.11a/b/g range.

Hence, the problem of dual-band oscillators for 5.2/6.8 GHz WLAN has been taken. The design has been made using a new category of semiconductor based switched resonator dual-band oscillator with radiating element, to demonstrate their utility in this specific wireless application.

1.4   Statement of Problem

The investigations reported in this dissertation are aimed to:

(a) Develop a switched resonator based dual-band oscillator for 5.2 GHz and 6.8 GHz frequencies.

(b) Develop a dual-band oscillator using semiconductor switch for 5.2 GHz and 6.8 GHz frequencies.

(c) Integration of oscillator with planar radiating element for wireless applications.

1.5   Organization of the Dissertation

This dissertation is organized as follows:-

Chapter 1 deals with the literature survey of the research work reported on Dual Band Oscillator (especially Switched resonator) and Oscillator type Active Integrated Antenna.

Chapter 2 presents a brief description of basic oscillator design techniques. This includes feedback oscillator theory, design of a two port negative resistance oscillator using a reflection coefficient method, important oscillator characteristics. Methodology for designing an oscillator including selection of transistor, DC analysis, biasing circuit, transistor stability, impedance matching networks design, HB analysis and matching optimization were discussed.

Chapter 3 describes detailed design and development of switched resonator dual-band oscillator for 5.2/6.8 GHz WLAN application starting from DC analysis to fabrication of the circuit.

Chapter 4 deals with the development of semiconductor based switched resonator dual-band oscillator using Schottky diode as a switch. This includes the bias network design to nonlinear analysis and finally results compared with the fabricated prototype.

Chapter 5 deals with the oscillator type active integrated antennas (AIA) concept. This includes the development of oscillator for 5.2 GHz frequency in which microstrip antenna works as frequency selective network. Finally development of semiconductor based switch resonator dual-band oscillator integrated with patch antenna is discussed.

Finally, *Chapter 6* summarizes a conclusion/discussion of the work done and suggests scope for future work on the CAD assisted dual-band oscillator with radiating element used in the dissertation.

Fundamentals of Oscillator Design

2.1   Introduction

This chapter begins by introducing the basics of an oscillator, concept of negative resistance, its important characteristics and basics of microstrip Patch Antenna. Finally, explain the detailed methodology for designing of an oscillator for developing a general procedure.

2.2   Basic Principle

Oscillators are essential part of the electronic circuitry. They occur in many applications and make possible circuits and subsystems that perform very useful functions. They can be termed as DC-to-RF converters or infinite- gain amplifiers [28]. Oscillations occur sometimes even when we don't desire them. Amplifiers can oscillate, if stray feedback paths are present. One of the simplest ways to view an oscillator is as an amplifier with a high-Q filter as a feedback network. This is commonly referred to as the feedback oscillator model as shown in Fig. 2.1. Broadband noise is present everywhere in the circuit. The amplifier boosts the signal level of the noise at all frequencies. This amplified noise then travels through the feedback loop back to the input of the amplifier.
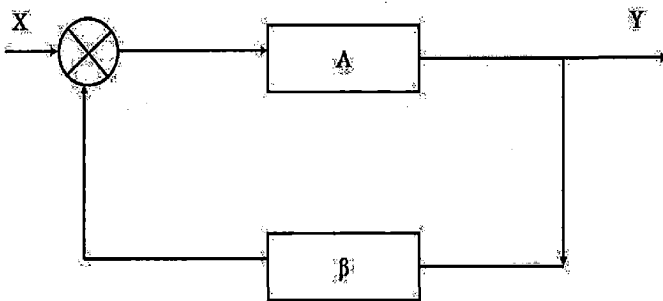
Fig. 2.1 Block diagram of a feedback system

The feedback loop consists of a band pass filter that allows the signal of the desired frequency. This frequency passes through the amplifier and filter repeatedly. A sinusoidal signal centered on the frequency of the filter which begins from the noise as the signal travels around the loop many times. The amplitude of this signal cannot grow infinitely. The bias circuit or the characteristics of the device used as the amplifier will limit the final amplitude. The transfer function of the forward-connected subsystem is A, while the feedback path has a subsystem with its transfer function as β. Therefore,

$$Y = A(X + \beta Y) \tag{2.1}$$

The closed-loop gain T (called the transfer function) of this system is found from this equation as

$$T = \frac{Y}{X} = \frac{A}{1 + A\beta} \tag{2.2}$$

and the phase shift

$$\arg[A\beta] = 180^0 \tag{2.3}$$

Product Aβ is known as the loop gain has a phase shift of 180^0 at some frequency ω_0. It is a product of the transfer functions of individual blocks in the loop. A is called the forward path gain. For a unity loop gain transfer function T becomes infinite. Hence Oscillation occurs when an amplifier is furnished with a feedback path that satisfies two conditions:

1. Amplitude Condition - The cascaded gain and loss through the amplifier / feedback network must be greater than unity.
2. Phase Condition - The frequency of oscillation will be at the point where loop phase shift totals 360 (or zero) degrees.

In most oscillator circuits, oscillation builds up from zero when power is first applied, under linear circuit operation. However, limiting amplifier saturation and other non-linear effects end up keeping the oscillator's amplitude from building up indefinitely. Thus, oscillators are not the simplest devices in the world to accurately design simulate or model.

Oscillator circuits are used for generating the periodic signals that are needed in various applications. These circuits convert a part of DC power into periodic output and do not require a periodic signal as input. Solid-state oscillators use a diode or a transistor in conjunction with the passive circuit to produce sinusoidal steady-state signals. Transients or electrical noise triggers oscillations initially. This process requires a nonlinear active device.

Since the device is producing RF power, it must have a negative resistance. An oscillator is fundamentally a nonlinear circuit and difficult to analyze. An oscillator consists of an amplifier (a negative resistance device that generates power), a resonator that store energy and control the frequency and a coupling circuit that delivers the power to load and a feedback circuit at a desired frequency and acceptable power-added efficiency (RF power out/DC power in). The efficiency of a low-noise oscillator varies, depending upon frequencies and configurations between 10% and 70%. In most cases the efficiency is a secondary problem. The primary task is to have a signal which is stable, free of spurious signals (clean), with low phase noise, and of sufficient level.

2.3   Concept of Negative Resistance

Generally microwave FETs are made up of GaAs because the electron mobility is greater than that of silicon used as a negative resistance device. Further improvement in performance of GaAs microwave transistor has been obtained using hetrojunction chip structure known as a high electron mobility transistor (HEMT). In the HEMT the electrons travel in the thin n-type AlGaAs layer drop completely into the GaAs layer to form a depleted AlGaAs layer. The hetero-junction created by different band-gap materials forms a quantum well in the conduction band on the GaAs side where the electrons can move quickly without colliding with any impurities because the GaAs layer is undoped, and from which they cannot escape. The effect of this is to create a very thin layer of highly mobile conducting electrons with very high concentration, giving the channel very low resistivity (or to put it another way, "high electron mobility").

The ideal inductors and capacitors store electrical energy in the form of magnetic and electric fields respectively. Since there is no loss in this system, the inductor recharges the capacitor back and the process repeats. Oscillations die out because of these losses. If a negative resistance can be introduced in the loop, the effective resistance becomes zero. In other words if a circuit can be devised to compensate for the losses, oscillations can be sustained. RF current starts flowing through the circuit at a frequency at which the imaginary parts of both impedances will cancel each other. This RF current causes the value of negative resistance to change unless the oscillation condition $-R_n = R_1$ is satisfied. Fig. 2.2 shows a one-port negative-resistance oscillator [10]. Z_{in} is the input impedance of the active device.
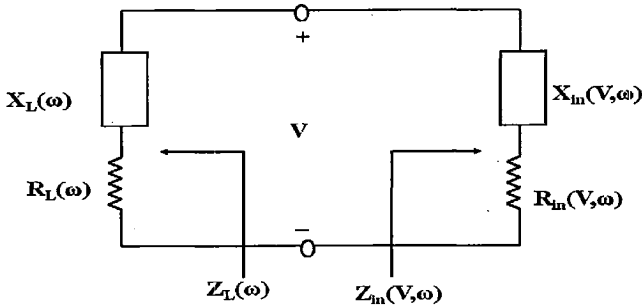
Fig. 2.2 Equivalent circuit for one-port negative resistance microwave oscillators

This impedance is current (or voltage) dependent as well as frequency dependent. Which we can indicate by writing

$$Z_{in}(V,\omega) = R_{in}(V,\omega) + jX_{in}(V,\omega).$$ (2.4)

The device is terminated with passive load impedance

$$Z_L(\omega) = R_L(\omega) + jX_L(\omega).$$ (2.5)

Applying Kirchhoff's Voltage Law (KVL) gives

$$(Z_{in}(V,\omega) + Z_L(\omega)) = 0$$ (2.6)

The one - port network is stable if

$$[\mathrm{Re}[Z_{in}(V,\omega) + Z_L(\omega)]] > 0$$ (2.7)

2.3.1 Oscillation Condition:

For the startup of oscillation negative resistance of the active device in a series circuit must exceed the load resistance by about 20% (i.e. $R_{in} = -1.2R_L$).

$$R_{in}(V,\omega) + R_L(\omega) = 0$$ (2.8)

$$X_{in}(V,\omega) + X_L(\omega) = 0$$ (2.9)

Initially, it is necessary for the overall circuit to be unstable at a certain frequency (i.e., the sum of R_L and R_{in} is a negative number).

$$|R_{in}(V,\omega)| > R_L(\omega)$$ (2.10)

Any transient excitation or noise then causes the oscillation to build up at a frequency ω. Since the load is passive, $R_L > 0$ and (2.8) indicates that $R_{in} < 0$. Thus while a positive

resistance implies energy dissipation a negative resistance implies an energy source. The condition of (2.10) controls the frequency of oscillation. For the stability of an oscillator high-Q resonant circuits such as cavities and dielectric resonators are used

2.3.2 Microwave Transistor Oscillator

The design procedure described here is general and applies to any transistor circuit configuration as long as its S-parameters are known. Unlike the amplifier circuit, the transistor for an oscillator design must be unstable. In a transistor oscillator a negative-resistance is effectively created by terminating a potentially unstable transistor with impedance designed to drive the device in an unstable region. The oscillator converts DC power to RF power using the negative resistance characteristics of active devices. Both Bipolar Junction Transistor (BJT) and GaAs Field Effect Transistor (FET) can be used to design a dual-band oscillator. However GaAs MESFET is preferred as they provide better noise characteristics [5]. Typically common source or common gate GaAs FET configurations are used (common emitter or common base for bipolar devices), often with positive feedback to enhance the instability of the device. For the dual band oscillator design we will modify the load matching (frequency selective network) as shown in Fig. 2.3 by dotted lines. The actual power output port can be on either side of the transistor. A resonator or frequency selective circuit is connected to the tuning port to give a desired resonator reflection coefficient Γs. The most common resonators are lumped element, distributed element (microstrip or coaxial line), Cavity, dielectric resonator, YIG, and varactor. All of these structures can be made to have low losses and high quality factor [4].
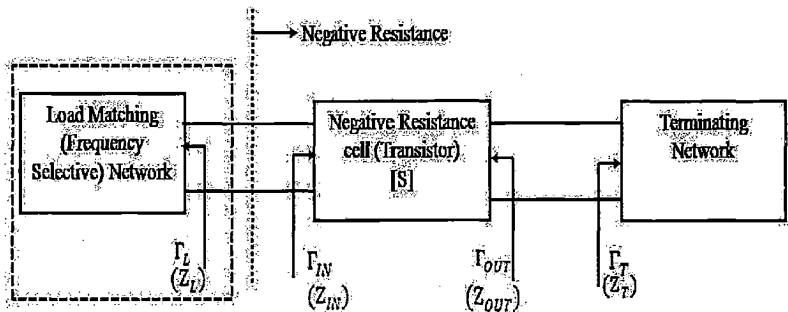
Fig. 2.3. Block diagram of microwave transistor based oscillator

Dual band oscillator is based on the negative resistance concept using a common-source series feedback element to generate the negative resistance. The HEMT is used in a network with source series feedback, successfully generating negative input impedance at the gate. At the input of this network, two microstrip resonators are coupled to define the frequency and conditions for oscillation. Then the output network is designed for optimum output power efficiency to the 50 Ohms load at both the frequencies. First the transistor configuration is selected so that the output stability circle can be drawn in the Γ_T plane, and Γ_T is selected to produce a large value of negative resistance at the input to the transistor [5]. Then the load impedance Z_L can be chosen to match Z_{in}. R_L will become less negative as the oscillator power builds up. Thus, it is necessary to choose R_{in} so that $R_{in} + R_L < 0$. Otherwise oscillation will cease when the increasing power increases R_{in} to the point where $R_{in} + R_L > 0$.

In practice a value of

$$R_L = \frac{R_{in}}{3} \tag{2.11}$$

is typically used. The reactive part of Z_L is chosen to resonate the circuit,

$$X_L = -X_{in} \tag{2.12}$$

For steady-state oscillation at the input port, we must have $\Gamma_{IN}\Gamma_L = 1$ or $\Gamma_{OUT}\Gamma_T = 1$. If the stability parameter K is not less than unity an external positive feedback can be used to make the device unstable. If $\Gamma_{in}\Gamma_L = 1$ or $\Gamma_{out}\Gamma_T = 1$ conditions satisfy than passive terminations Z_L and Z_T must be added for resonating the input and output ports of the active device at the frequency of oscillation. Input port is oscillating when

$$\Gamma_L\Gamma_{in} = 1 \tag{2.13}$$

Where

$$\Gamma_L = \frac{1}{\Gamma_{in}} = \frac{1 - S_{22}\Gamma_T}{S_{11} - \Delta\Gamma_T} \tag{2.14}$$

$$\because \Gamma_{in} = S_{11} + \frac{S_{12}S_{21}\Gamma_T}{1 - S_{22}\Gamma_T} \tag{2.15}$$

and

$$\Gamma_T = \frac{1 - S_{11}\Gamma_L}{S_{22} - \Delta\Gamma_L} \tag{2.16}$$

But $\qquad \Gamma_{out} = S_{22} + \dfrac{S_{12}S_{21}\Gamma_L}{1 - S_{11}\Gamma_L} = \dfrac{S_{22} - \Delta\Gamma_L}{1 - S_{11}\Gamma_L}$ $\qquad\qquad$ (2.17)

$$\therefore \Gamma_{out}\,\Gamma_T = 1 \qquad\qquad (2.18)$$

Thus the conditions for oscillations are satisfied at both ports if they are satisfied at one port. An output matching of the oscillator has been designed using single stub matching technique based on the load calculated using equation (2.11) as shown in Fig. 2.3.

Next, plot the input stability circle to choose a reflection coefficient for the input matching network. The center and radius of the input stability circle are computed respectively based on the formulas given below.

$$Rin = \left| \frac{S_{12}S_{21}}{|S_{11}|^2 - |\Delta|^2} \right|$$

$\qquad\qquad$ (2.19)

$$C_{in} = \frac{\left(S_{11} - \Delta S_{22}^{\;*}\right)^{*}}{\left(|S_{11}|^2 - |\Delta|^2\right)}$$

$\qquad\qquad$ (2.20)

Where

$$\Delta = |S_{11}S_{22} - S_{12}S_{21}| \qquad\qquad (2.21)$$

And for output stability circle, the radius and center of the circle ar computed as follows.

$$R_{out} = \left| \frac{S_{12}S_{21}}{|S_{22}|^2 - |\Delta|^2} \right|$$

$\qquad\qquad$ (2.22)

$$C_{out} = \frac{\left(S_{22} - \Delta S_{11}^{\;*}\right)^{*}}{\left(|S_{22}|^2 - |\Delta|^2\right)}$$

$\qquad\qquad$ (2.23)

Dual band oscillators have been conventionally comprehended by reconfiguring the frequency selective network. Typically, a negative resistance cell is combined with a switch-controlled resonator. In a two-port oscillator, the frequency selective network or passive part determines the generated frequency depending on the resonance frequency of the network, while the active core of the circuit provides enough negative resistance at this resonance frequency to compensate for the loss of the tank.

2.4   Important Oscillator Characteristics [4]

2.4.1   Phase Noise of an Oscillator

In frequency synthesizer applications today, active circuits are often used to satisfy system requirements and to sustain oscillations in a lossy LC-tank oscillator. The random electronic noise associated with these active circuits causes uncertainties in the synthesizer output, and part of the uncertainties is considered phase noise. Phase noise can be defined as the random timing fluctuation in an oscillator period. Oscillators do not generate perfect signals. The various noise sources in and outside of the transistor modulate the VCO resulting in energy or spectral distribution on both sides of the carrier. Phase noise is mathematically modeled as random phase modulation. It is measured in dBc/Hz at offset as shown in Fig. 2.4. Phase noise is generally specified in dBc/Hz at a given offset frequency for a particular carrier. Therefore, phase noise can be found by measuring the ratio of the power spectral density (1-*Hz* bandwidth) at a given offset frequency to the total power at the carrier frequency.
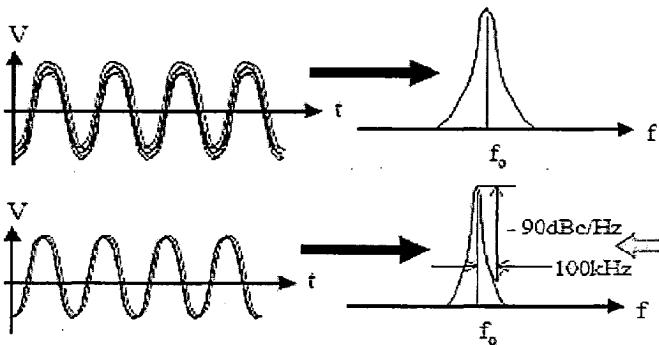
Fig. 2.4 Phase noise representation [10]

The power spectrum of a synthesizer output with phase noise is shown in Fig. 2.5. The basic process creating oscillations is by feedback using a resonant circuit with period current pulses charging the tuned circuit. Between charging pulses, the transistor conducts zero current and is considered 'off.' Phase noise is produced depending on the shape of the current pulse when the transistor is 'on.' If the current is a relatively narrow pulse and existing for very short time. There will be less phase noise produced than with a wider and longer

pulse. The narrow pulse provides less contribution to creating time shifts in the energy storage when lined up with the output waveform peak. Only pulse width need be considered in design because the feedback process automatically synchronizes the current pulse with the output waveform peak. The pulse width can be designed into an oscillator using nonlinear design techniques, thus gaining control over transistor noise sources affecting phase noise.
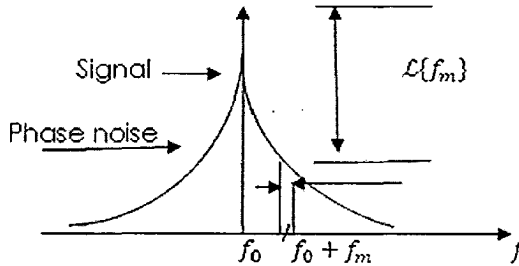
Fig. 2.5 Signal and phase noise spectrum of an oscillator [5]

Sources of Noise - The roots of phase noise lie in the noise sources of the transistor (or other active device) used in the oscillator. The PM noise is directly effects the frequency stability of the oscillator and related noise sidebands. There is a limited control over the noise sources in a transistor, only being able to control the device selection and bias point. Shot noise, burst noise, partition noise, thermal noise and $1/f$ noise are the major transistor noise sources. All of these noise sources except thermal noise exist only when current is flowing in the device.

This can be controlled to some extent by controlling the current duty cycle. Thermal and shot noises are the two fundamental sources of noise for an RF oscillator. At any temperature above absolute zero, thermal agitation causes electrons in any conductor or semiconductor to be moving at random. Thermal noise is expressed as either a current or voltage associated with a resistance. In transistors, each of the emitter, base, and collector currents paths will have its own associated shot noise. The final noise source, $1/f$ noise, also called flicker noise, is not a broadband phenomenon like thermal and shot noise. The nonlinear performance of oscillators transforms this low frequency $1/f$ noise by up-conversion into the near-sideboards of the fundamental oscillation signal [29]. Because the high frequency components of that noise are attenuated by the resonator, noise processes that generate low frequency components are of most concern. Oscillator noise models noise

prediction using Leeson's model [30] is based on the time-invariant properties of the oscillator such as resonator Q, feedback gain, output power, and noise figure. If we combine the Leeson formula with the tuning diode contribution, the following equation allows us to calculate the noise of the oscillator completely [30].

$$\mathcal{L}(f_m) = 10\log\left\{\left[1 + \frac{f_o^2}{(2f_m Q_L)^2}\right]\left(1 + \frac{f_c}{f_m}\right)\frac{FkT}{2P_{sav}} + \frac{2kTRK}{f_m^2}\right\} \tag{2.4}$$

Where $\mathcal{L}$ (f_m) is ratio of sideband power in a 1Hz bandwidth at f_m to total power in dB. The limitation of this equation is that the loaded Q in most cases has to be estimated, as does the noise factor. The microwave harmonic-balance simulator, which is based on the noise modulation theory (published by Rizzoli) [31], automatically calculates the loaded Q and the resulting noise figure, as well as the output power [32]. The second model is an improvement on Leeson's model, was proposed by Lee and Hajimiri is based on the nonlinear time-varying (NLTV) properties of the oscillator current waveform. The phase noise analysis is based on the effect of the noise impulse on a periodic signal.

Method of Reducing Phase Noise - To reduce phase noise the following point to be adopted.

1.   By reducing the current flow through the device will lead to lower noise levels. Narrowing the current pulse width in the active device will decrease the time that noise is present in the circuit.

2.   Choose an active device that has a low flicker corner frequency (1/f). Phase noise can be lowered by selecting a transistor with low flicker noise, resonator configuration with a high Q, selecting a transistor with a low-noise figure value at the operating input and avoiding saturation of the transistor.

3.   Noisy power supplies may cause additional noise. Power supply induced noise   may be seen at offsets from 20 Hz to 1 MHZ from the carrier. If the VCO is powered from a regulated power supply, the regulator noise will increase depending upon the external load current drawn from the regulator. Phase noise can also be caused by noise originating in the power supply or coupled to the dc bias circuits power supply filtering should not be overlooked as a means to minimize phase noise.

2.4.2   Frequency Range

The output frequency of a VCO can vary over a wide range. The frequency range is determined by its tuning circuit. The use of a very high f_T device may lead to problems with

stability. The frequency of operation determines the active device to be used as well as the technology.

2.4.3   Output Power

The output power requirement is determined by the type of application. The use of a high power device will degrade the phase noise performance. In other words more the output power more will be phase noise. Practical designs require one or more isolation stages between the oscillator and the output. VCO output power is usually measured into a 50 ohm load. The VCO output power can vary as much as ±2 dB over the tuning range. A typical output level is 0 to +10 dBm.

2.4.4   Harmonic Suppression

Non-linear device will create harmonics at multiples of the fundamental frequency. These harmonics may interact with out-of-band signals in the system mixer causing spurious responses in the receiver. In transmitters the efficiency may be reduced if strong signals are generated that are not required. These results in the total power shared amongst the different signals generated. The oscillator/VCO has a typical harmonic suppression of more than 15 dB. For high-performance applications a low-pass filter at the output will reduce the harmonic contents to a desired level.

2.4.5   Sensitivity to Load Changes

Many wireless applications use a VCO alone to keep manufacturing costs down. This avoids the buffering action of a high reverse-isolation amplifier stage. In such applications frequency pulling the change of frequency resulting from partially reactive loads is an important oscillator characteristic. Pulling is commonly specified loading or in terms of the frequency shift when connected to a load. This is because of a non unity VSWR (such as 1.75, usually referenced to 50Ω) compared to the frequency that results with a unity-VSWR load (usually 50Ω).

A buffer at the output is necessarily to isolate the VCO from any output load variations (pulling) to provide the required output power. Meeting simultaneously the output power and load pull specification directly with a stand-alone oscillator would be difficult. This buffer amplifier requires a higher supply current. Alternative would include using at the output circulators, isolators or passive attenuators.

2.5   Topologies of Dual Band Oscillators

Oscillators are also considered as DC-to-RF converters. A typical oscillator consists of an active device, a passive frequency-determining resonant element and matching element. The active device can be a two-terminal device like a Gunn or IMPATT diode or more commonly a three-terminal device including a junction bipolar transistor, metal semiconductor FET or more recent devices using newer semiconductor materials. In order to generate a high frequency signal an active device with sufficient gain to compensate for feedback loop losses is necessary. Oscillation conditions need to be satisfied for the circuit containing the active device and passive element. Two different topologies are used for this purpose, as shown in Fig.2.6 in their generalized form [4].
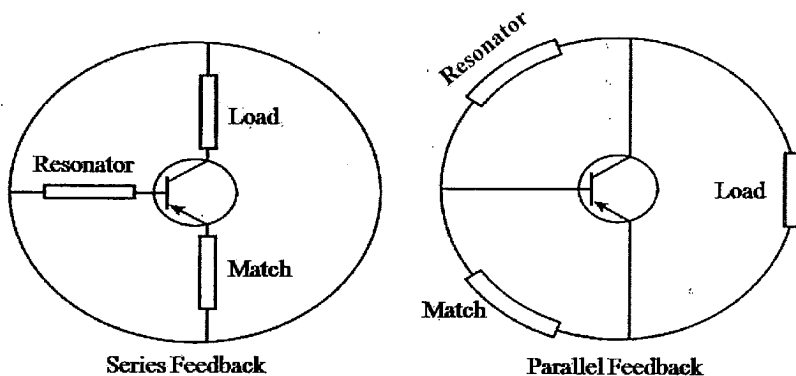
Fig. 2.6 Oscillator design topologies using three–terminal devices

A series feedback oscillator is the one used for higher frequencies, where as a parallel feedback oscillator is the one in which the frequency-determining element is used as a feedback element between the input and output in order to generate necessary instability and a negative resistance oscillator is the one in which reflection gain at a given terminal is used to satisfy the oscillation condition when connected to a frequency-determining element with the proper phase condition.

Dual band oscillators have been conventionally comprehended by reconfiguring the frequency selective network. Typically, a negative resistance cell is combined with a switch-controlled resonator. In a two-port oscillator, the frequency selective network or passive part

determines the generated frequency depending on the resonance frequency of the network, while the active core of the circuit provides enough negative resistance at this resonance frequency to compensate for the loss of the tank. The dual band oscillator topology of HEMT based Switched resonator oscillator for dual band operation is shown in Fig. 2.7.
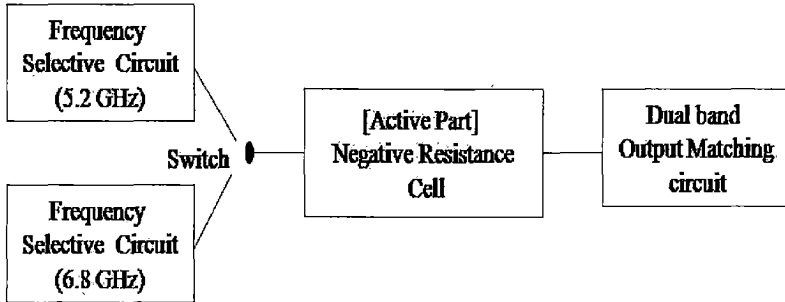
Fig. 2.7 Conceptual diagram of switched resonator based dual band oscillator

We have used HEMT based negative resistance oscillator for 5.2/6.8 GHZ frequencies. Concept of switched resonator is used to change the desired frequency band. Micro- switch or semiconductor switch can be used for above purpose.

2.6   *Methodology for Designing Oscillators*

2.6.1. DC Analysis

The first and foremost step in the dual band oscillator design is to perform a DC analysis to verify the operating   point of the Amplifier [5]. The DC analysis automatically checks the topology of the circuit and finds the solution iteratively such that the sum of all DC currents into each circuit node is zero. Biasing of the oscillator as it directly affects the simulation. Biasing can have a negative effect on the overall performance if implemented poorly. Thus, the appropriate operating point is chosen depending on the kind of application chosen for the desired results.

2.6.2. Bias Network Design

A good DC biasing is used to select the proper quiescent point and hold the quiescent point constant over variations in transistor parameters and temperature. Junction field-effect transistor device-to-device parameter variation is generally greater than for bipolar junction

transistors. There are very simple JFET biases schemes exist which are suitable for many applications. With these schemes, active bias is guaranteed, but the device operating bias point may vary over a wide range from device to device. There are many ways of biasing a transistor to obtain the necessary operating point as discussed briefly below:

Grounded Source - One simple scheme is to DC ground the gate and source. The drain current that flows is *Idss* and is somewhat independent of the drain - source voltage, when Vds is greater than VP, the pinch-off voltage. *VP* is generally a few volts. Idss in a typical RF JFET varies over an order of magnitude range from device to device. Device selection allows tighter specification of *Idss*. *Idss* decreases with increasing temperature.

Resistor divider network - In this method two separate power supplies for gate and source will be required. In practice, the gate supply is usually a fixed DC voltage source varied by employing an appropriate resistor divider network to supply the required gate voltage. The source is grounded in this case. The maximum gain is obtained from a JFET when the source is grounded and hence, this is preferred if a high efficiency is required.

Self-bias network - The self-bias scheme develops a negative gate-source voltage equal to the voltage dropped in the source resistor; Rs. Increasing source current develops greater negative gate-source bias which inhibits the increasing source current. A source bypass capacitor is placed in parallel with the resistor to prevent the RF signal from loading the transistor i.e. the RF signal at the operating frequency sees a short to the ground via the bypass capacitor. This scheme therefore provides a degree of bias stabilization. The resulting drain current, Id, is less than Idss. The major advantage of this biasing is that only a single positive supply is needed to power up the transistor.

An active bias network - This circuit uses another FET to maintain the main FET at the desired operating point. This analog circuit prevents any change in the FET Q-point by adjusting itself to provide the required gate bias. Any changes in the Q-point cause the network to determine the gate voltage to be supplied to bring the Q-point back to its original intended position.

A bias Tee Bias Tees are required to supply DC voltages and currents to RF devices such as FETs etc. The main job of this kind of biasing is to avoid power supply loaded with the RF frequency and to avoid the shift of the operating point of the transistor. The basic schematic of a bias tee is shown in Fig. 2.10 to understand its operation better.
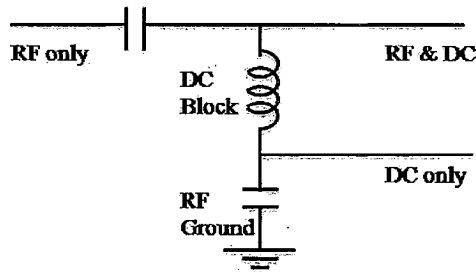
Fig. 2.10: Typical bias tee network [28]

The DC block capacitor prevents any stray DC voltages or currents from entering the circuit which might cause problem. The ideal case would be that the RF sees an open circuit at the bias network. In case any RF signal passes through the inductor (RF choke) it sees a short to the ground via RF ground capacitor shown above. On the other hand, the applied DC sees an open circuit to the ground and pass through the inductor which acts as a Short.

In microstrip implementation, the inductor could be replaced by a high impedance line and the capacitor can be implemented as an open or radial stub. The length of the high impedance line representing the inductance is kept (λ/4) so that the RF signal sees the open stub as a capacitor shorted to ground. The only disadvantage of this bias network is that is occupies a relatively large area. Therefore, in a microstrip implementation this bias network may look as shown if Fig. 2.11. This is a commonly used bias circuit and its performance parameters are RF bandwidth, insertion loss and mismatch at the two RF ports and the maximum DC current depending on the device being used as specified on the manufacturer's datasheet. We will use this biasing for our design.

Fig. 2.11. Microstrip implementation of bias tee network [5]

2.6.3. Transistor stability

There are two types of feedback; negative feedback and positive feedback. For positive feedback the gain will increase, which is useful for peaking the gain at the upper band edge or for making high-frequency oscillators [5]. Also a positive feedback is used to obtain an input reflection coefficient module greater than unity in input port o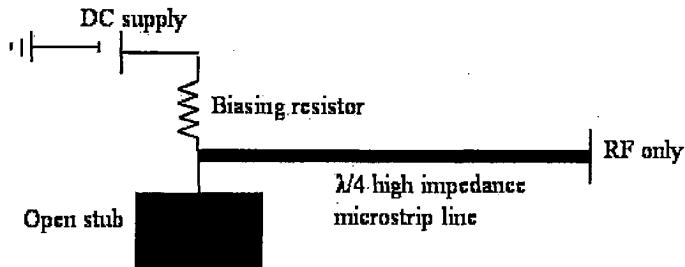f the device. For the greater the unity for $|S_{11}|$, which gives guarantee that the oscillations will be initiated and the active device's oscillatory process will be maintained. In a transistor oscillator a negative-resistance is effectively created by terminating a potentially unstable transistor with impedance designed to drive the device in an unstable region. Unlike amplifier for an oscillator we require a device with a high degree of instability [4]. To check the transistor instability, the transistor is biased at the chosen operating point using the selected biasing network. The S-parameters of the transistor are then measured at this operating point. The conditions for transistor to be unstable are:

$$K < 1 \tag{2.25}$$

$$\text{and} \qquad |\Delta| < 1 \tag{2.26}$$

$$K = \frac{1 - |S_{11}|^2 - |S_{22}|^2 + |\Delta|^2}{2|S_{12}S_{21}|} \tag{2.27}$$

$$\Delta = S_{11}\,S_{22} - S_{12}\,S_{21} \tag{2.28}$$

The transistor has to be unstable in the entire desired frequency range of operation.

2.6.4. Impedance Measurement and Matching Networks design

A matching network circuit is not only designed to meet the requirement of minimum power loss but it is also based on additional constraints, such as minimizing the noise influence, maximizing power handling capabilities, and linear frequency response. The simplest possible type of matching network is two-component network (L-sections) due to their element arrangement. These networks use two reactive components to transform the load impedance Z_{Load} to the desired impedance Z_L.

Two methods can be used to design matching network (i) analytically (ii) using smith chart as graphical design tool [10]. Once the transistor has been stabilized in the desired frequency range at the fixed operating point, the next step is to design the matching network. We will use a microstrip line matching network consisting transmission lines followed by shunt stubs. The microstrip transmission line matches the real part of the transistor load

impedance to the output port, while the imaginary part of the load impedance is cancelled out by the shunt stub [5]. The transmission line realizing the stub is normally terminated by a short or by an open circuit. At one of the two ports of the transistor is called the terminating matching network and the one at the other port is called the load-matching network as shown in Fig. 2.3.

The terminating matching network is used to provide the proper termination so that the transistor presents a negative-resistance at the the port (i.e., the load port), which is designed to satisfy the oscillation conditions. If an active device is used to supply an amount of energy equal to the energy dissipated, the circuit can sustain oscillations. The actual power output port can be on either side of the transistor. Typically common source or common gate FET configurations are used (common emitter or common base for bipolar devices), often with positive feedback to enhance the instability of the device. After the transistor configuration is selected the output stability circle can be drawn in the Γ_T plane, and Γ_T selected to produce a large value of negative resistance at the input to the transistor. Then the load impedance Z_L can be chosen to match Z_{IN}. R_L will become less negative as the oscillator power builds up it is necessary to choose R_{in} so that $R_{in} + R_L < 0$. Otherwise oscillation will cease when the increasing power increases R_{IN} to the point where $R_{in} + R_L > 0$. This has already been discussed while explaining the concept of negative resistance.

2.6.5. HB Analysis and Matching Optimization

The final step in Oscillator design is carrying out HB analysis for observing the different characteristics like output frequency, its harmonics and phase noise etc [34]. This also helps in optimizing the input and output matching networks if required, for bringing the matching elements values and hence, their implementation into realms of practical realization.

2.7   Conclusions

We have discussed the basic principle of oscillator and concept of negative resistance including basic of HEMT, oscillation condition. A few important characteristics oflike phase noise and power added efficiency is also described. Finally the summary of oscillator design steps is given in the following steps for a transistor oscillator.

1.   Select a potentially unstable transistor at the frequency of oscillation. If not, use feedback elements to make it unstable.

2.   Design the terminating network, Z_T or Γ_T, to make $\left|\Gamma_{OUT}\right| > 1$ >1 by choosing Z_T or Γ_T in the unstable zone of the stability circle.

3.   From Z_T and the transistor small signal S–parameter, calculate   and confirm $\left|\Gamma_{OUT}\right| > 1$. Choose the load according to the oscillating condition as $X_L(f_o) = -X_{OUT}(f_o)$ and $R_L(f_o) = -\dfrac{1}{3}\left|R_{OUT}(0, f_o)\right|$. The chosen value for Z_L usually produces a working oscillator.

The measured oscillation frequency will be shifted from the design value, since   ( ), used in determining f_o, is assumed to be independent of the amplitude. Design the load matching network to transform a 50 Ω load to Z_L. The steps to be followed sequentially to design and analyze an oscillator can be summarized as shown in Fig. 2.12.
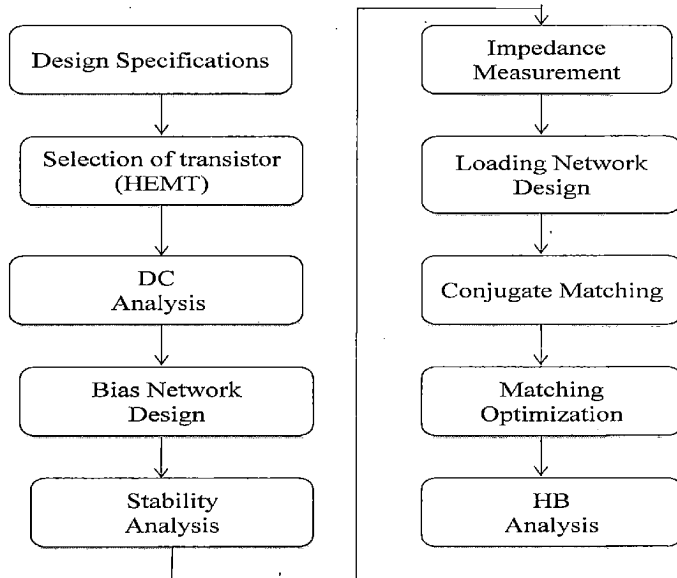
Fig. 2.12 Summarized oscillator design steps.

Switched Resonator Dual Band Oscillator

3.1   Introduction

This chapter starts with the design of switched resonator dual band oscillator for 5.2/6.8 GHz WLAN applications. Initially dual band oscillator characteristics were determined with the help of circuit simulation and the parameters obtained in this simulation were used as the starting point of the full wave e.m simulation. The implementation of electrical parameters obtained by circuit simulation was carried out using microstrip techniques. The full wave nonlinear analysis using combined use of circuit and e.m simulation predicts the desired characteristics of the oscillator.

3.2   DC Bias Simulation and Bias Network Design:

First step of oscillator design is the specifications of the proposed dual band oscillator [Fig. 2.12]. Design specifications of the dual band oscillator are given below:

Desired frequency of oscillation   : 5.2 and 6.8 GHz

Desired output power at both the frequency : > 0 dBm

Desired phase noise at both the frequency   :   Below -130 dBc/Hz at an offset of
                                                 1MHz from the carrier.

Second step is selection of microwave a suitable active devices. GaAs FET generally has better noise figures and can operate at much higher frequencies (in excess of 100 GHz) [5]. At the present time, GaAs metal semiconductor FET (GaAs MESFET) is the most popular choice for microwave applications above 3 GHz. It's an important active device for use in microwave analog and high-speed digital integrated circuits [33]. Si-doped AlGaAs FET NE4210S01 is selected for our design, since its operating frequency is from 2 to 18 GHz [35]. Next step is to provide a good *DC* biasing to select the proper quiescent point and hold the quiescent point constant over variations in transistor parameters and temperature.

Moreover, *S*-parameters of the transistor depend upon the DC bias circuit provided to the transistor and vary with the transistor bias network. First of all, a DC-bias quiescent point was selected from the transistor DC-bias curves, as per the design requirements.

Simulation set up for the measurement of the DC characteristics of the HEMT in ADS is shown in Fig. 3.1. Next, Si-doped AIGaAs FET NE4210S01(datasheet attach as Appendix C) was selected from the installed Spice model for NEC Active transistor library, and placed in the schematic window. FET Curve tracer template was inserted in the schematic and the maximum rating for V_{ds} was selected as 4V (as per the datasheet) and for I_{ds} it was set to be 20 mA.
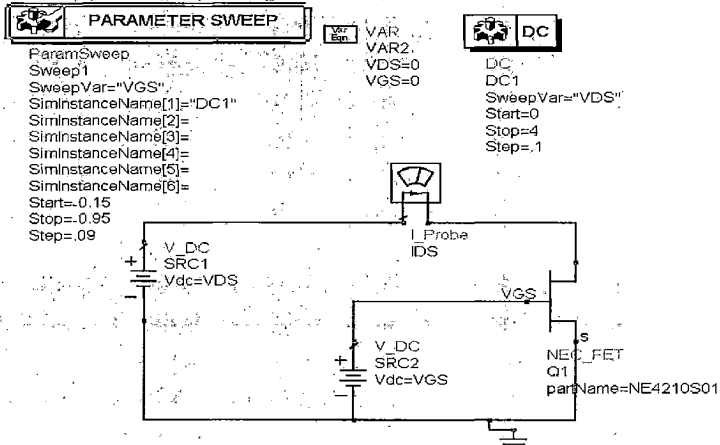

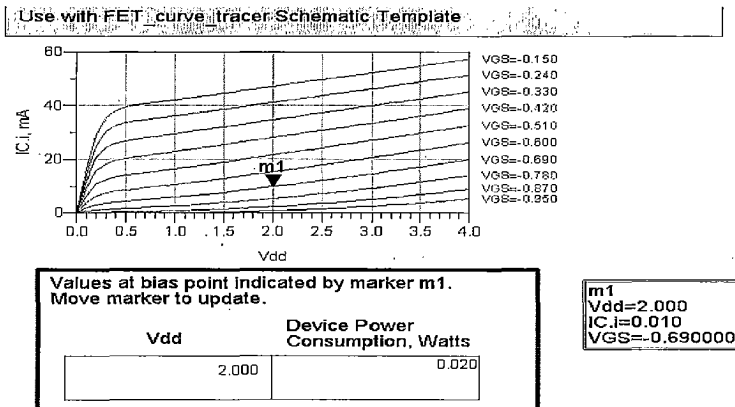**Fig. 3.1. Schematic view for DC simulation of a transistor.**

Fig. 3.2. Bias point selection from resulting DC output characteristic curves of the FET.

DC Bias Simulation was performed in ADS using the model for the transistor. A DC bias point for oscillator design was selected to be about half of the maximum ratings as V_{DS}=2V and I_{DS}=10mA (V_{GS}=-0.69V). The DC characteristics are shown in Fig. 3.2.

A bias Tee biasing circuitry was selected for the DC bias of HEMT, as biasing techniques discussed in Chapter 2. It consists of the high impedance (selected as 130Ω) λ/4 wavelength (with electrical length 90^0) microstrip line followed by a shunt low impedance (taken as 20Ω) λ/4 wavelength electrical length 90^0 open stub. The dimensions are calculated using linecalc tool in ADS as shown in the following section.

Table 3.1
Microstrip Line dimensions for 5.2 GHz Bias network

Z_0 (Ohms)	W (mm)	L (mm)
130	0.418194	9.294850
20	12.534100	8.211310

The bias network designed for 6.8 GHz is similar to 5.2 GHz except for the dimensions. The dimensions of the bias network and measured S-parameters are shown in Table 3.2.

Table 3.2
Microstrip Line dimensions for 6.8 GHz bias network

Z_0 (Ohms)	W (mm)	L (mm)
130	0.425754	7.084260
20	12.687300	6.240640

We have taken the following dimension after non linear analysis for the biasing circuit which meets the requirement for both the frequencies.

Table 3.3
Microstrip Line dimensions for combined Dual band bias network

Z0 (Ohms)	W (mm)	L (mm)
130	0.418194	6.29485
20	12.63393	6.240640

3.3   *Stability analysis and S-parameter Simulation:*

After the design of DC Bias Network S-Parameter Simulation was performed for the stability analysis of the transistor and for obtaining the S-parameters which would be used for further analysis. A feedback capacitor was added at source to get the unstability. The Stability factors K for a HEMT for 5.2 GHz and 6.8 GHz is given as

$$K = \frac{1 - |S_{11}|^2 - |S_{22}|^2 + |\Delta|^2}{2|S_{12}S_{21}|} = -0.467 \, and -0.226$$

$$(3.1)$$

Where Δ is given by

$$\Delta = |S_{11}S_{22} - S_{12}S_{21}|$$

$$(3.2)$$
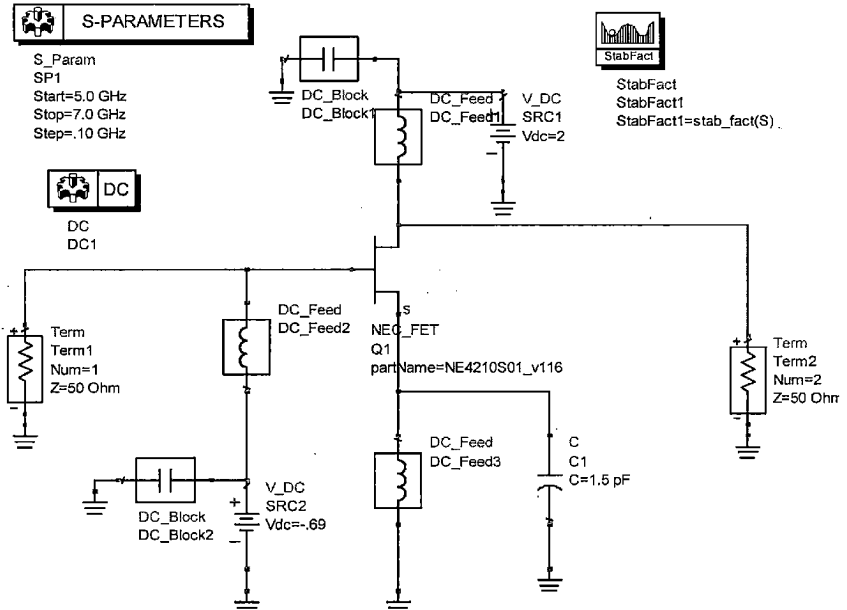
Fig. 3.3. Schematic view for S-Parameter simulation of the transistor.

As discussed in Chapter 2 a dual-band oscillator will be unstable if the following two conditions are satisfied.

$$K < 1 \qquad (3.3)$$

$$\Delta < 1 \qquad (3.4)$$

The two-port representation of feedback transistor circuit may be analyzed using *S*-parameters [5]. From the analysis of the stability factor the transistor was obtained to be potentially unstable at this frequency as shown in the Fig. 3.3 and 3.4.

freq	S(1,1)	S(1,2)	S(2,1)	S(2,2)	StabFact1
5.000 GHz	1.906 / -43.386	0.235 / 55.035	6.463 / 175.509	1.473 / -50.012	-0.496
5.100 GHz	1.935 / -45.796	0.244 / 52.987	6.660 / 172.503	1.485 / -52.288	-0.482
5.200 GHz	1.962 / -48.295	0.252 / 50.860	6.853 / 169.424	1.495 / -54.646	-0.467
5.300 GHz	1.988 / -50.881	0.260 / 48.654	7.042 / 166.275	1.504 / -57.083	-0.452
5.400 GHz	2.011 / -53.552	0.268 / 46.374	7.226 / 163.057	1.511 / -59.598	-0.437
5.500 GHz	2.031 / -56.303	0.276 / 44.022	7.402 / 159.775	1.515 / -62.185	-0.422
5.600 GHz	2.049 / -59.129	0.283 / 41.605	7.569 / 156.432	1.518 / -64.842	-0.407
5.700 GHz	2.063 / -62.025	0.290 / 39.128	7.725 / 153.036	1.517 / -67.562	-0.392
5.800 GHz	2.074 / -64.984	0.297 / 36.597	7.869 / 149.593	1.514 / -70.338	-0.377
5.900 GHz	2.081 / -67.997	0.303 / 34.023	7.999 / 146.112	1.508 / -73.162	-0.362
6.000 GHz	2.083 / -71.055	0.308 / 31.413	8.114 / 142.600	1.500 / -76.026	-0.347
6.100 GHz	2.082 / -74.150	0.313 / 28.778	8.213 / 139.067	1.488 / -78.920	-0.332
6.200 GHz	2.076 / -77.270	0.318 / 26.128	8.295 / 135.524	1.473 / -81.835	-0.316
6.300 GHz	2.066 / -80.406	0.321 / 23.474	8.358 / 131.982	1.455 / -84.760	-0.301
6.400 GHz	2.051 / -83.547	0.324 / 20.825	8.404 / 128.449	1.435 / -87.686	-0.286
6.500 GHz	2.033 / -86.683	0.326 / 18.194	8.432 / 124.937	1.411 / -90.601	-0.271
6.600 GHz	2.010 / -89.803	0.328 / 15.589	8.441 / 121.455	1.386 / -93.498	-0.256
6.700 GHz	1.984 / -92.900	0.328 / 13.020	8.434 / 118.013	1.358 / -96.366	-0.241
6.800 GHz	1.955 / -95.965	0.329 / 10.495	8.411 / 114.618	1.328 / -99.198	-0.226
6.900 GHz	1.923 / -98.991	0.328 / 8.023	8.372 / 111.278	1.297 / -101.9...	-0.210
7.000 GHz	1.889 / -101.9...	0.327 / 5.609	8.320 / 107.999	1.264 / -104.7...	-0.195

Fig. 3.4. Resulting S-Parameters of FET with biasing circuit

3.4   Design of Matching Network

Once S-parameter has been obtained at both the frequencies, next design step was impedance matching network design. The S-parameters obtained at the designing frequency of 5.2 GHz are:

$$
\left.
\begin{aligned}
S_{11} &= 1.962 \angle -48.30^0 \\
S_{12} &= 0.252 \angle 50.86^0 \\
S_{21} &= 6.853 \angle 169.42^0 \\
S_{22} &= 1.495 \angle -54.64^0
\end{aligned}
\right\}
$$

(3.5)

Two methods can be used to design matching networks viz (i) analytically and (ii) using smith chart as graphical design tool [10]. The design of matching circuit wii be carried out using both the methods at both frequencies. For the common source with series capacitive feedback S-parameters, the input and the output stability circles are drawn on the smith chart, using smith chart utility in Advanced Design System (ADS), as shown in Fig. 3.5. Same can be checked analytically on smith chart as discussed in Chapter 2. The input stability circle is a contour in the source plane that indicates source termination values that will make the

output reflection coefficient have a unity magnitude. An output reflection coefficient less than unity will indicate a stable device, while an output reflection coefficient greater than unity indicates a potentially unstable device.
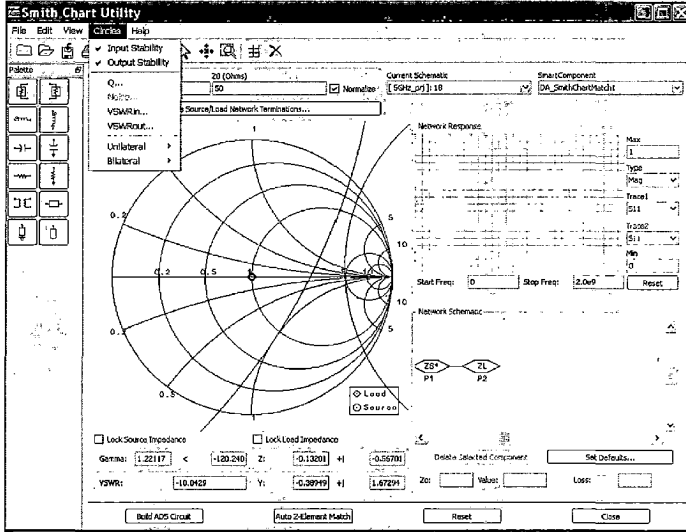

Fig. 3.5. Input and output stability circles for 5.2 GHz case.

As seen from Fig. 3.5. great deal of flexibility is avaliable in selection of the reflection coefficient for the input matching network. Theoritically, any Γ_S residing inside of the stability circle would satisfy our requirements, because S_{11} and S_{22} are greater than 1. In practice, however, one has to choose Γ_S in such a way that it maximizes the output reflection coefficient. Values of reflection coefficients are calculated in such a way that it satisfies oscillation condition as shown in chapter 2. The calculated value of reflection is given below:

$$
\left.
\begin{aligned}
\Gamma_{IN} &= 2.462\angle - 48.3^0 \\
\Gamma_{out} &= 4.758\angle - 52.65^0 \\
\Gamma_L &= 0.4061\angle 48.3^0 \\
\Gamma_T &= .210\angle 52.65
\end{aligned}
\right\}
$$

(3.6)

Now the output matching circuit was designed using the Smith Chart utility available in ADS by utilizing using the obtained S-Parameters, as shown in Fig. 3.6. The output matching circuit can be obtained analytically and with the help of smith chart found to be the same as obtained from smith chart utility. The designed matching network contains the 50Ω microstrip line with electrical length 24.58^0 and the 50Ω open circuit stub with electrical length 157.5^0(as shown in Fig. 3.7.).
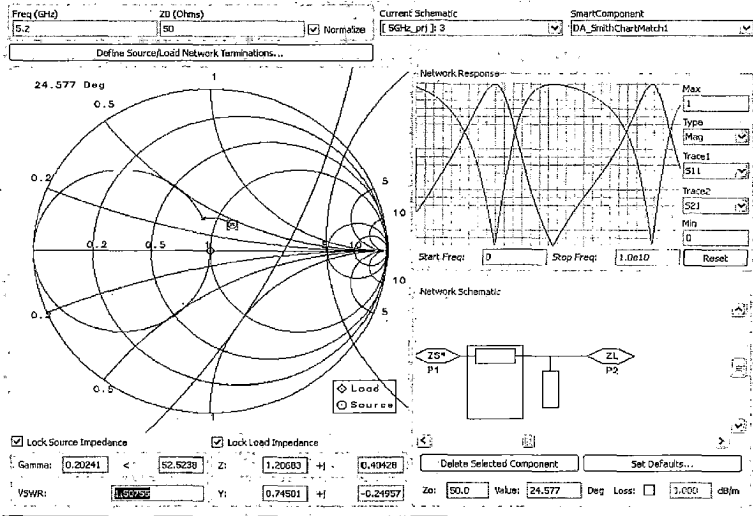

Fig. 3.6. Matching network design using smith chart utility in ADS
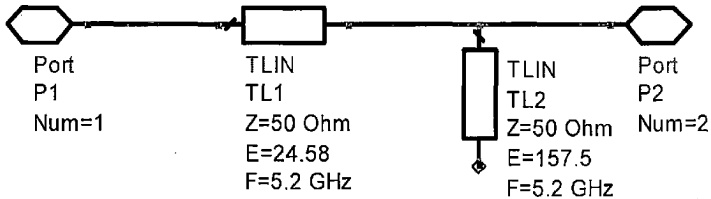

Fig. 3.7. Resulting matching network dimensions for 5.2 GHz case.

The conversion of the electrical parameters of the transmission lines into physical dimensions was done using LineCal tool in the ADS. The dimensions of the lines are

computed for a NH9338 substrate having ε_r =3.38 and 1.524 mm thickness (15 to 18 μm copper thickness, dissipation factor of 0.0025) are summarized as shown below in table.3.4.

Table.3.4
Dimensions of the microstrip transmission lines in matching Circuit.

Transmission line Characteristic impedance	Electrical Length	Width, mm	Length, mm
50Ω	24.58^0	3.557980	2.373140
50Ω	157.5^0	3.557980	15.206200

At the input port while looking into amplifier input impedance is given by

$$Z_{In} = 50 \times \frac{1 + \Gamma_{IN}}{1 - \Gamma_{IN}} = -66.84 - j48.55 \tag{3.7}$$

and loading impedance is given by

$$Z_L = 22.28 + j48.55 \tag{3.8}$$

At the output port while looking into amplifier output impedance is given by

$$Z_{OUT} = 50 \times \frac{1 + \Gamma_{OUT}}{1 - \Gamma_{OUT}} = -60.56 - j21.17 \tag{3.9}$$

This inductive impedance will be resonating input port which performs matching as well as resonator or frequency selective circuit. Similarly we will calculate output matching circuit and loading impedance for 6.8 GHz frequency.

$$\left.\begin{aligned} S_{11} &= 1.955\angle -95.965^0 \\ S_{12} &= 0.329\angle 10.50^0 \\ S_{21} &= 8.411\angle -114.62^0 \\ S_{22} &= 1.328\angle -99.20^0 \end{aligned}\right\} \tag{3.10}$$

Reflection coefficient obtained from the S-parameters which satisfies oscillation condition is given below.

$$\left.\begin{aligned} \Gamma_{IN} &= 2.2455\angle -95.965^0 \\ \Gamma_{out} &= 4.080\angle -111.8^0 \\ \Gamma_L &= 0.407\angle 93.142^0 \\ \Gamma_T &= .245\angle 110.15 \end{aligned}\right\} \tag{3.11}$$

The negative resistance behaves as capacitor, hence input port resonates. Now adding the source impedance ($Z_L = 48.55\ \Omega$) at the input port (i.e. at gate terminal) and the matching network at the output port (i.e. at the drain terminal) of the transistor, the final circuit drawn is shown in Fig. 3.8.
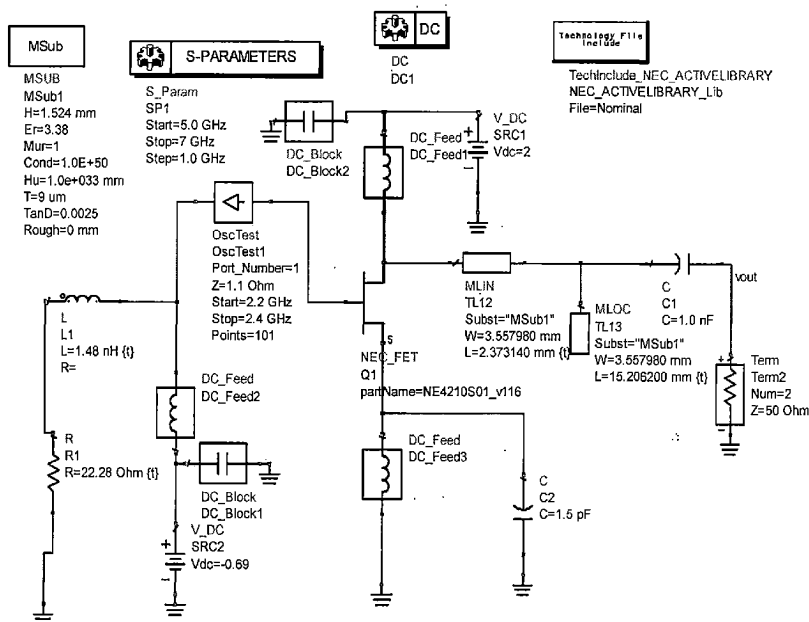

Fig. 3.8. Schematic view for S-Parameter simulation of the oscillator.

The load impedance for 6.8 GHz is given by $Z_L = -11.11 + j32.39$. At the output port while looking into amplifier output impedance is given by $Z_{OUT} = -37.83 - j18.32$. The biasing voltage at source and gate, are maintained to be Vdd=2V and Vgs= -0.69 V. The simulated results can be obtained using ADS. OscTest is an ADS probe component used to evaluate the loop-gain associated with a circuit. The OscTest probe component and its three-port S parameter values is basically a three-port circulator with port one excited by the incident wave, and with ports 2 and 3 defined by the reflection coefficients respectively. Since the magnitude is greater than 1 and the phase is zero at 5.2 GHz and 6.8 GHz frequencies, hence oscillation will occur at both the frequencies as shown in Fig. 3.9.

freq (5.000GHz to 7.000GHz)
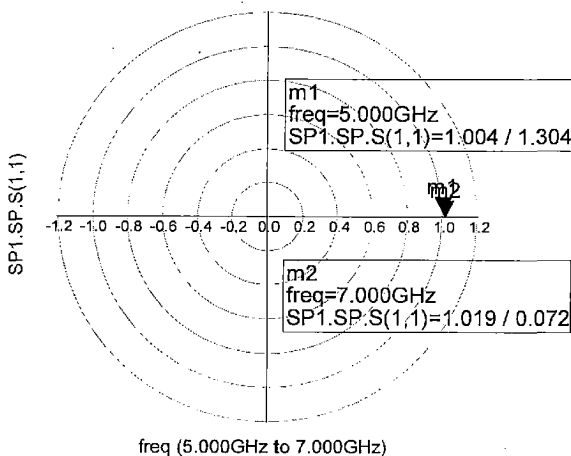
Fig. 3.9. S-parameter simulation results.

The next step of the design is to replace some of the circuit elements with microstrip lines, specifically the tuning capacitor, shunt inductor and RF bias circuits (as shown by the DC_Feeds).

(1)   Calculate 1.48 nH inductor as an open-circuit stub.

Reactance $X_L = 2\Pi.f.L = 48.55\Omega$

$X_L = Z_0 \tan \Theta + 90$ (OPEN Circuit Stub)

$X_L = Z_0 \tan \Theta$ (SHORT Circuit Stub)

Where $\Theta < 90^0$ ($90^0 \lambda_{op} / 4$)

Rearrange to get Θ ie $\Theta = \tan\text{-}1(X_L / Z_0) + 90 = 28.68 + 90 = 134.16^0$ (for 130Ω line)

(2)   Calculate 1.5 pF capacitor as an open-circuit stub.

$\omega C = 2\Pi.f.C$

$\omega C = \tan \Theta / Z_0$

$\Theta = 67.80^0$

Where $\Theta < 90^0$ ($90^0 \lambda_{op} / 4$)

(3)   DC_Feed

Use 90 degree 130 ohm lines.

(4)   DC_Capacitor shunts

Use 90 degree 20 ohm lines.

The ADS model was updated to use 'ideal' microstrip lines and open-circuit stubs as shown in Fig. 3.10. The dimensions of the matching network were optimized to get the required frequency of oscillations for both the frequencies. Two different resonators or input matching circuit for both the frequencies were used.

In the ADS schematic of the oscillator, a TEE junction was used to connect the three components. Here, the TEE junction is the ideal connection of the three components with different connections. The microstrip line after the matching network (i.e., after TEE junction) is a 50Ω line does not affect the performance of the oscillator (i.e. frequency of oscillations, output power). The DC Block is a capacitor of 1 nF used to block the DC at the output of oscillator.
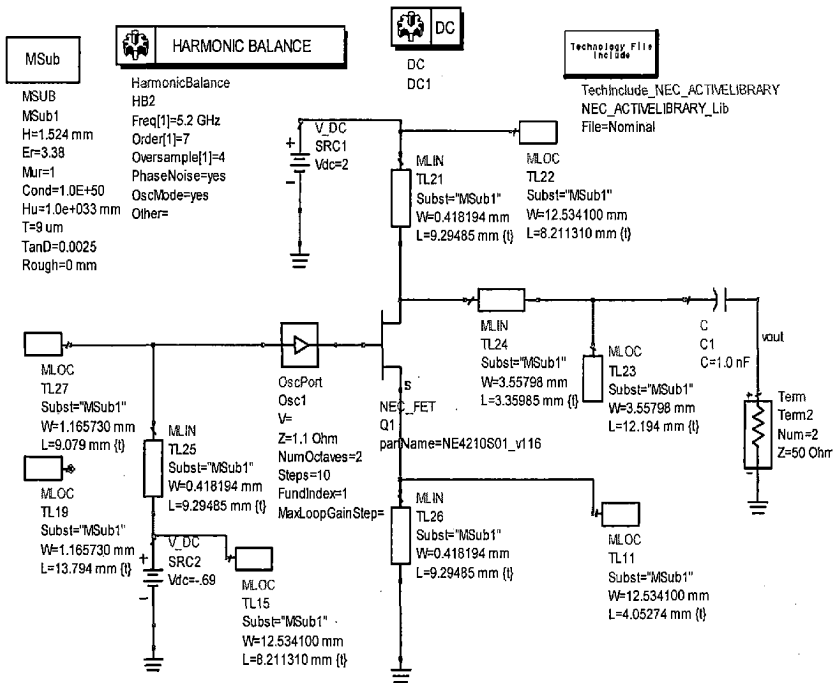

Fig. 3.10. Nonlinear analysis of microstrip line based dual band oscillator.

3.5   Harmonic Balance Simulation:

The next step was to perform a harmonic balance simulation to predict oscillator characteristics i.e. the output power spectrum and phase noise performance for both the frequencies. The harmonic balance simulator box is set to the following values:

Freq: 5.2 GHz and order 7, Noise (1): select log, start 10Hz, stop 100MHz and points per decade: 10, Noise (2): select "vout", select nonlinear noise. Select phase noise=yes, and set oversample at least 4. All the parameters left to their default values.

The schematic of the harmonic balance ADS simulation of the oscillator design is shown in Fig. 3.10. OscPort is an ADS probe component used to calculate the oscillator waveform using a harmonic-balance simulation. It calculates the large-signal steady state form of the oscillatory signal. The OscPort component should be inserted at the point where OscTest was used and a harmonic-balance simulator must be inserted in the program. Here, the "osc port" box is added at a position separating the output and negative resistance region. This box is used for checking the open loop gain of the oscillator. The resulting frequency spectrum and corresponding phase noise is shown in Fig. 3.11. and 3.12.
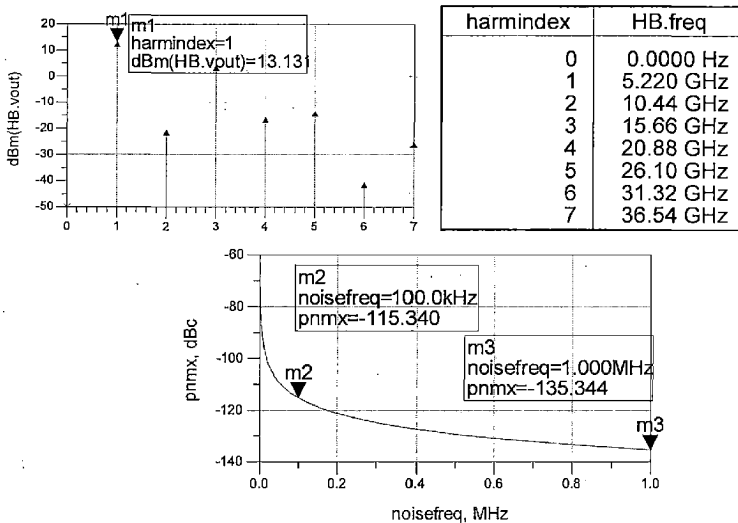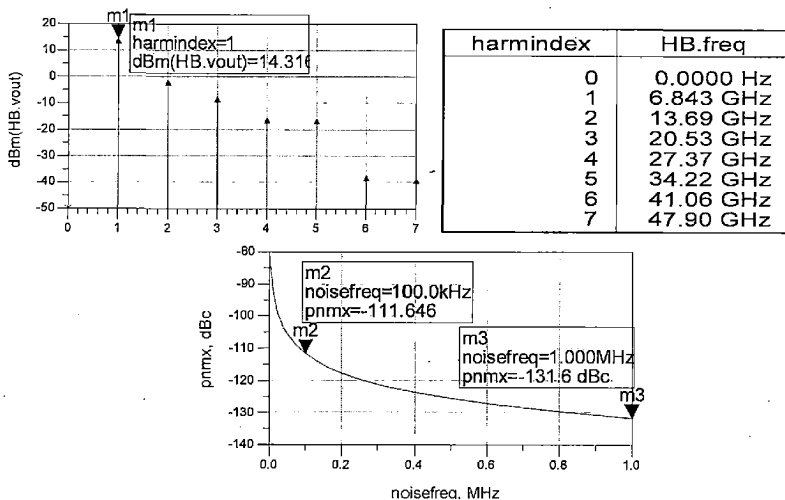

**Fig.3.11. Output power and phase noise predictions at 5.2 GHz.**

Fig. 3.12. Output power and Phase noise predictions at 6.8 GHz.

The output power of 13.13 dBm and phase noise of -115.34 dBc/Hz at an offset of 100 KHz at the fundamental frequency of 5.2GHz. The output power of 14.31 dBm and phase noise of -111.646 dBc/Hz at an offset of 100 KHz at the fundamental frequency of 6.8 GHz.

3.6   Non Linear Analysis of Dual Band Oscillator

Finally, non linear analysis using full wave simulation was carried out [37]. The layout without components has been drawn and simulation was done using ADS in conjunction with EMDS/Momentum to fine tune dimensions of the final layout. This layout was inserted in schematic as a component and connects all other component like the active device and power supply. Since full wave analysis is the most accurate form of analysis for such a design, it is set to include all the parasitic and stray losses that might occur in the circuit. In schematic we take all ideal components and no coupling effect were considered was taken. Whereas, in Momentum Simulation includes the effects due to coupling between the lines and other electromagnetic. The flow chart for full wave analysis is shown in Fig. 3.13. The dual band operation was achieved by using a switched resonator topology. Since the length of microstrip has to change micro-switch or membrane switch was used to select

the desired frequency band i.e. either 5.2 GHz or 6.8 GHz. This microstrip resonator absorbs the switch capacitance into the resonator, thus permits the use of large switches to diminish the Q degradation of the resonator tank due to the switch.
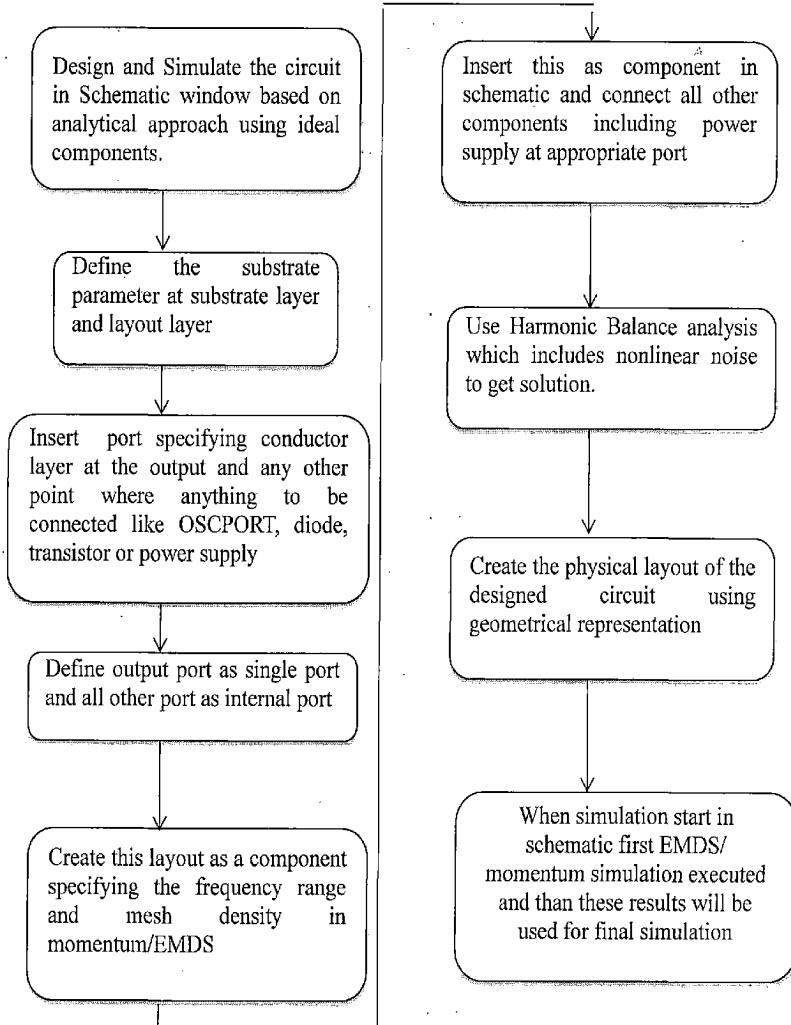
Fig. 3.13. Flow chart of full wave simulation of oscillator using EMDS/Momentum

The simulated layout of the switched resonator dual band oscillator for full wave analysis is shown in Fig. 3.14. Since the length of microstrip is changing micro-switch was used to select the desired frequency band i.e. either 5.2 GHz or 6.8 GHz. For 5.2 GHz switch is closed i.e. complete length of microstrip line will be considered and switch is open for 6.8 GHz frequency. Add layout component was drawn one by one in schematic to run co-simulation, because the output results obtained from the simulation of designed line lengths were not satisfactory at first. Further, an optimization approach was followed to get the desired output frequency obtained by manually changing the line lengths and simulations were repeated until a satisfactory output was obtained.
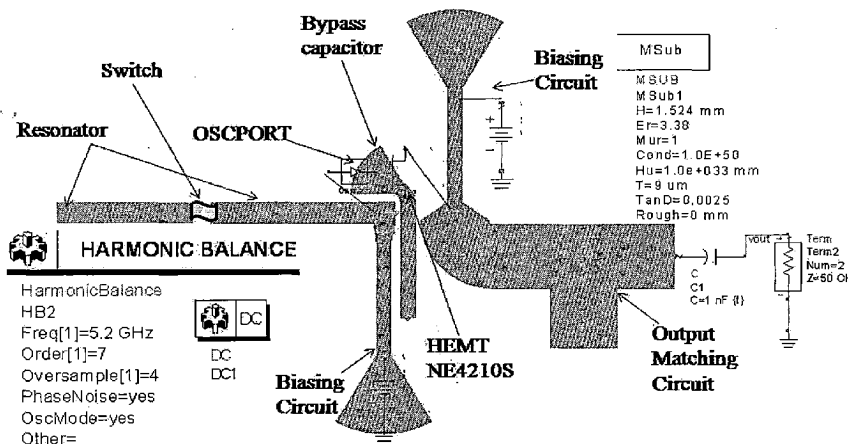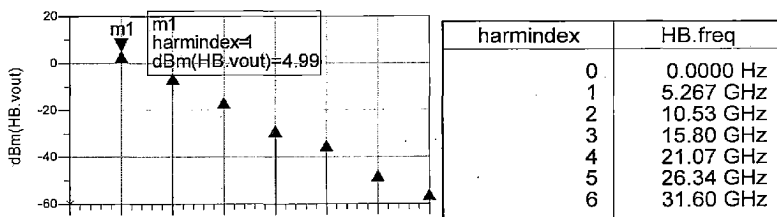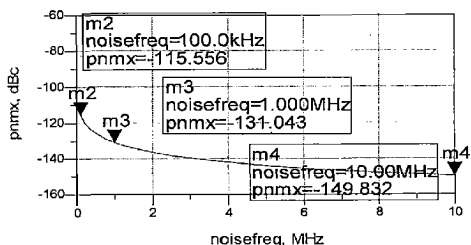

Fig. 3.14. Layout of the switched resonator dual band oscillator for full wave analysis.

The results obtained after optimization was obtained are shown in Fig. 3.15 and Fig. 3.16..

harmindex	HB.freq
0	0.0000 Hz
1	5.267 GHz
2	10.53 GHz
3	15.80 GHz
4	21.07 GHz
5	26.34 GHz
6	31.60 GHz

Fig. 3.15. Resulting output power and phase noise after full wave simulation at 5.2 GHz

The output power has been obtained as 4.99 dBm for 5.2 GHz frequency and 9.39 dBm for 6.8 GHz frequency, which is 7 dBm less as compared to the result obtained in circuit simulation.

harmindex	HB.freq
0	0.0000 Hz
1	6.893 GHz
2	13.79 GHz
3	20.68 GHz
4	27.57 GHz
5	34.47 GHz
6	41.36 GHz
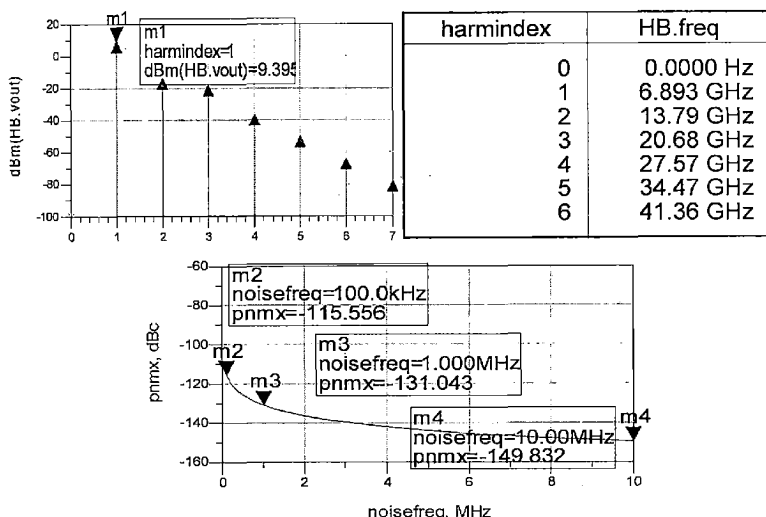
Fig. 3.16. Resulting output power and phase noise after full wave simulation at 6.8 GHz

3.7   Characterization of Fabricated Circuits

The fabricated prototype is shown in Fig.3.17. The dual band oscillator characteristics are measured on spectrum analyzer. The measured output power has been obtained as -1.89 dBm for 5.2 GHz frequency and 3.94 dBm for 6.8 GHz frequency as shown in Fig. 3.18 and

3.19. The output power for 5.2 GHz is less because of the membrane switch. The switch effect will be introduced and hence output at 5.2 GHz is less compared to simulated result. For 6.8 since only first part of resonator comes so the design goal was met. The measured phase noise and output power are within 5–10 % of predictions at 6.8 GHz frequency.
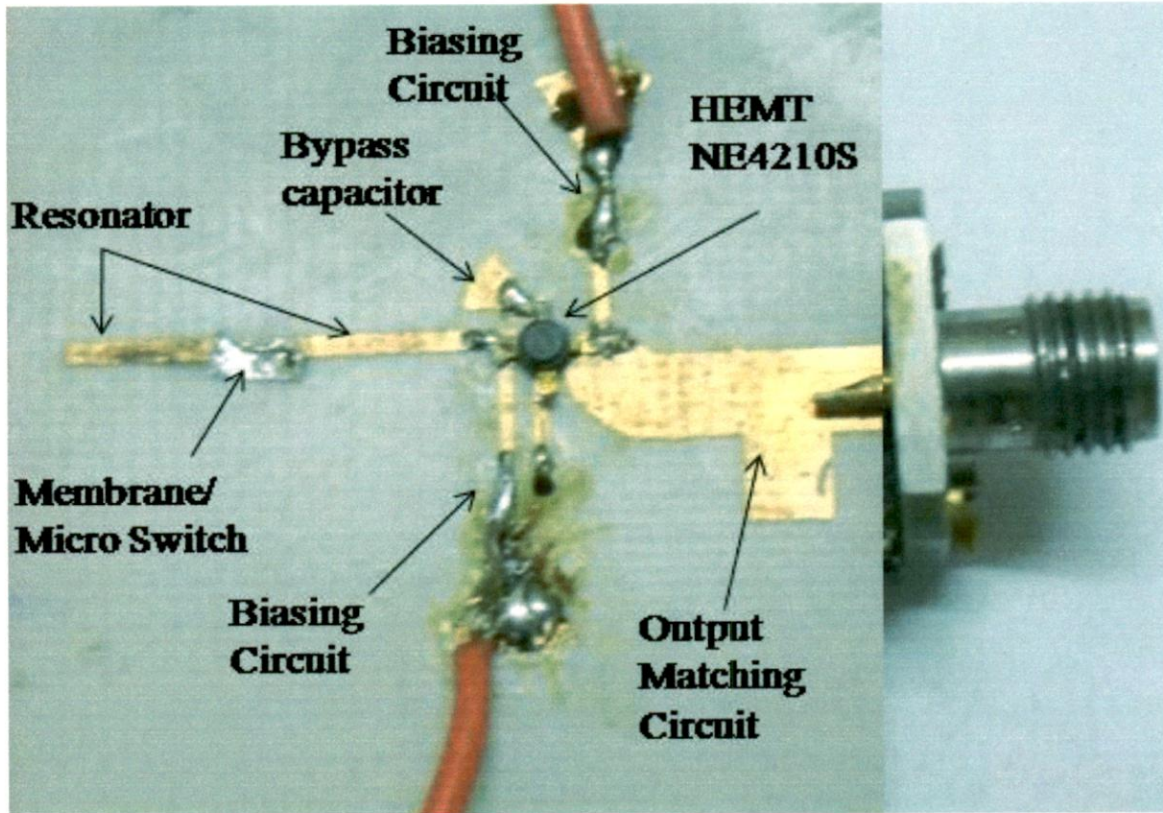

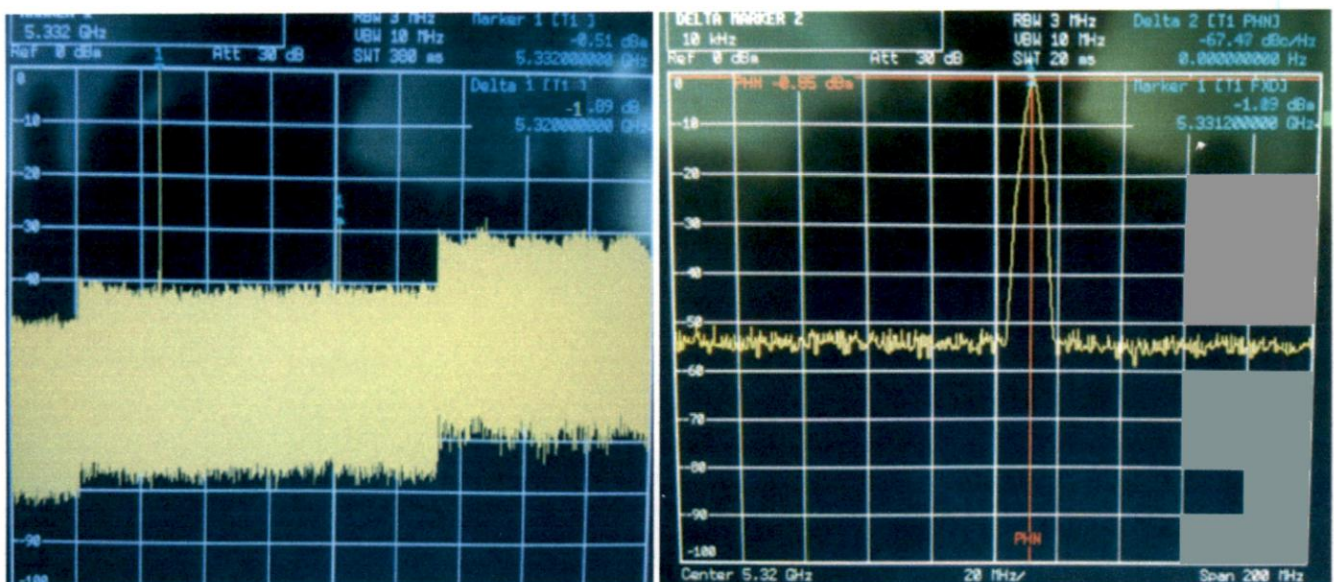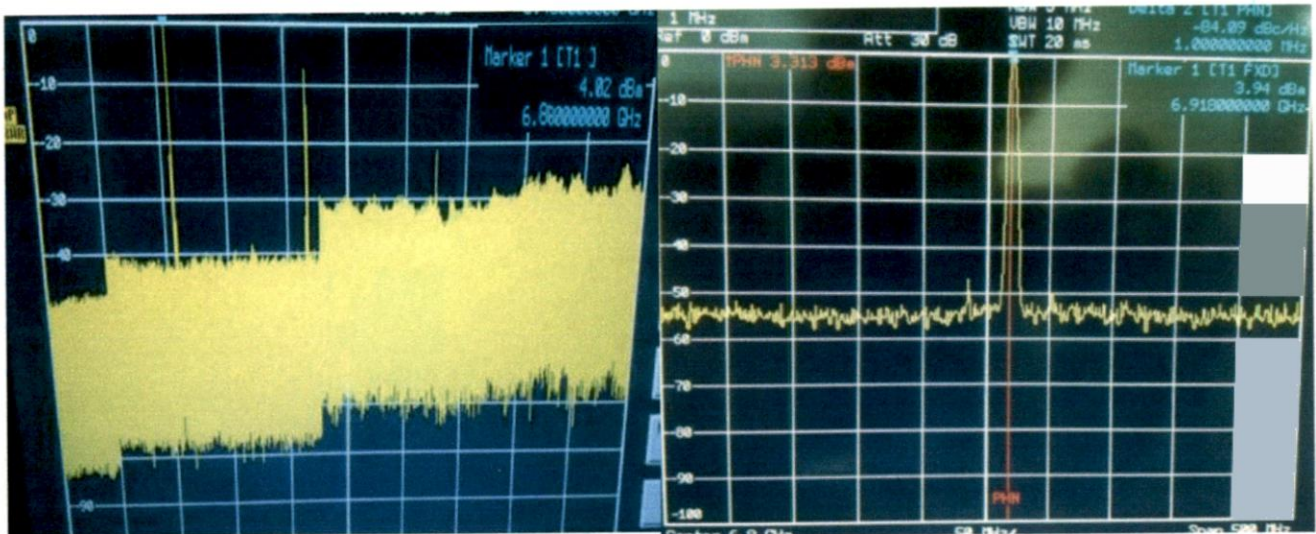**Fig. 3.17. Hardware prototype of switched resonator dual band oscillator.**

Fig. 3.18. Output power and phase noise on spectrum analyzer at 5.2 GHz

Fig. 3.19. Output power and phase noise on spectrum analyzer at 6.8 GHz

3.8   *Conclusions*

Nonlinear analysis of HEMT based Dual band Oscillator has been carried out using commercially available circuit simulator alone as well as circuit simulator in combination with electromagnetic simulator. The numerically obtained output power and phase noise of the fabricated prototype dual band oscillator from both methods are compared and as expected, results obtained from full wave nonlinear analysis differs from circuit simulation because circuit simulator ignores the effect of coupling between lumped and distributed elements. Hence, this full wave nonlinear analysis method can be used to design and accurately predict the behavior of dual band oscillator. This dual-band oscillator exhibited a phase noise of -67.47 dBc/Hz and -84.09 dBc/Hz at 100 KHz offset and output power of -1.01 dBm and 3.94 dBm operated near 5.2 GHz and 6.8 GHz respectively. Though this band-switching technique exhibits an outstanding feature of a simplified analog circuitry, miniaturized size, high performance, low cost (single transistor), low supply voltage, low power consumption, high power output yet the power output at 5.2 GHz frequency is very less when complete length of microstrip resonator comes in picture, compared to simulated one, because of micro switch. This problem can be overcome with the replacement of membrane switch to semiconductor switch shown in next chapter.

Semiconductor Switch Based Dual Band Oscillator

4.1   Introduction

Instead of micro-switch, the use of semiconductor switch for selection of frequency band will be discussed. A Schottky diode was used as a switch. In general, the first step involves selection of a diode that allows the operation at the maximum frequency of interest, which in our case is 7 GHz. As a thumb rule of design, a diode's cut-off frequency, should be greater than or equal to ten times the maximum frequency of operation of the circuit, i.e., 70GHz for our case. A diode's cut-off frequency is related to the zero-bias junction capacitance, and the series resistance, of the diode. Schottky Diode HSMS 286K from the built in SPICE model available in high frequency diode in ADS was selected. The specification sheet of Avago's surface mount microwave Schottky detector diode [38], HSMS 286K (SOT-363, 6pins), indicates the series resistance and the zero-bias junction capacitance values of 6Ω and 0.18-pF, respectively. The resultant cut-off frequency of 147.37-GHz meets the afore-mentioned requirement and, therefore, the diode was selected for implementing the semiconductor switches incorporation of the selected diode's model in ADS.

4.2   DC Bias Simulation and Bias Network Design:

The biasing condition for the HEMT was used in Chapter 3 (section 3.1). Now, the biasing condition for the Schottky diode will be determined. Ideal lumped component DC_feed and DC_Block for the biasing circuit of Schottky diode were used. Simulation set up for the measurement of the DC characteristics of the Schottky diode in ADS is as shown in Fig. 4.1. The model of the selected diode is available in the component library of ADS under the subheading of 'HF Diode Library'. The diode model, 'di_hp_HSMS286K_20000301' has selected datasheet attach as Appendix D to simulate its characteristics. A DC Bias Simulation was performed in ADS using the model for the Schottky diode. The resulting V-I characteristics for Schottky diode is shown in Fig. 4.2. The Schottky diode is operating as a switch. So Schottky diode will conduct or act a close switch

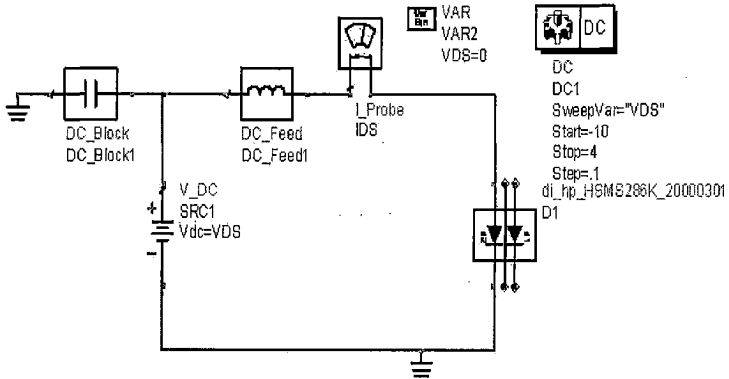at 0.3 V or above in forward bias and act as off or open switch below 0.3 V till -7.1 V before breakdown.

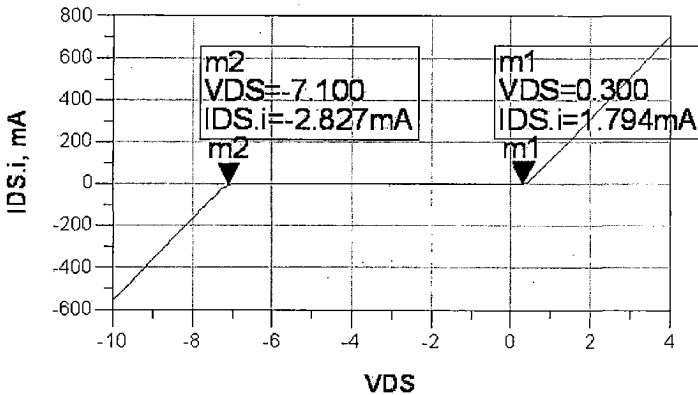**Fig. 4.1. Schematic view for DC simulation of the Schottky diode.**

**Fig. 4.2. Resulting V-I characteristics for the Schottky diode**

When ideal lumped components were replaced by the distributed one, the bias Tee biasing circuit is represented by a combination of the high impedance (130Ω) $\lambda/4$ wavelength (with electrical length 90^0) micro strip line followed by a shunt low impedance (20Ω) $\lambda/4$ wavelength electrical length 90^0) open stub for DC_feed and DC_block respectively as shown in Fig. 4.3. The dimensions were calculated in linecalc tool in ADS. The dimension for the biasing circuit for Schottky diode after optimization is shown in Table 4.1.

Table 4.1

Microstrip Line dimensions of bias network for Schottky diode (optimized)

Z_0 (Ohms)	W (mm)	L (mm)
130	0.418194	6.29485
20	12.63393	6.240640

4.3   S-parameter Simulation:

S-Parameter simulation was executed to predict the insertion loss and isolation provided by the Schottky diode. First of all, for the determination of insertion loss, the impedance offered by the Schottky diode looking from the input or anode side was determined. The layout of the biasing circuit was drawn and co-simulation was carried out for determination of impedance of the Schottky diode as shown in Fig. 4.3.
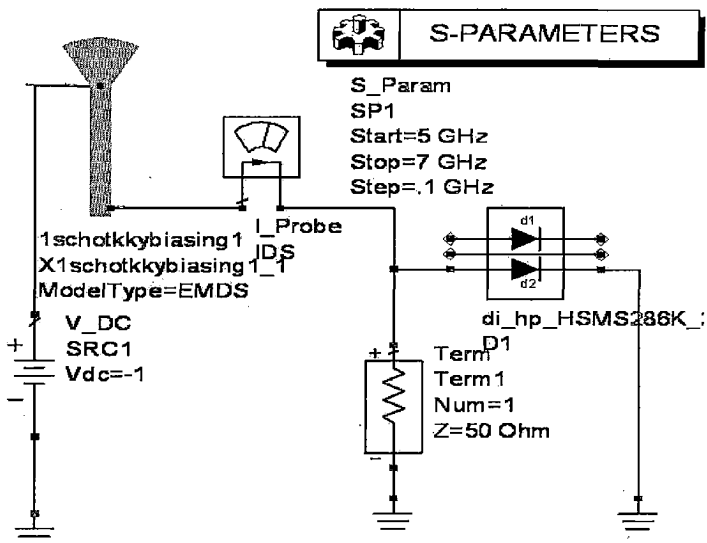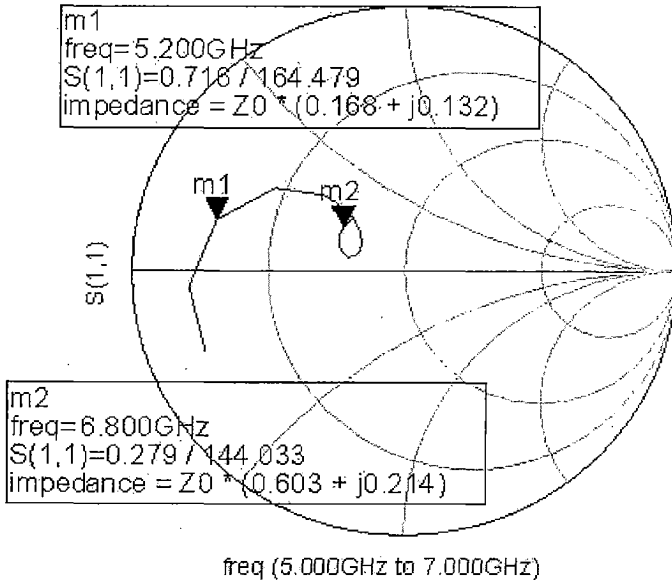

Fig. 4.3. Circuit setup of the Schottky diode for insertion loss measurement.

The value of the impedance offered by the Schottky Diode at both the frequencies is shown in Fig. 4.4. The insertion loss of the Schottky diode is given by

$$Insertion\_loss = 10\log\left[\left(1+\frac{R}{Z_0}\right)^2 + \left(\frac{X}{2Z_0}\right)^2\right]dB$$

(4.1)

The maximum value of insertion loss is 0.8 dB. To find out the isolation provided by Schottky diode when connected in circuit is accomplished by impedance offered from the cathode side. Ideally it should provide very high resistance when reverse biased.

m1
freq=5.200GHz
S(1,1)=0.718 /164.479
impedance = Z0 * (0.168 + j0.132)

m2
freq=6.800GHz
S(1,1)=0.279 /144.033
impedance = Z0 * (0.603 + j0.214)

freq (5.000GHz to 7.000GHz)

Fig. 4.4. Resulting input impedance of Schottky diode for circuit setup

The same could be found out by knowing the value of the S_{21}. The circuit arrangement for determining the S_{21} is shown in Fig. 4.5 The isolation for 5.2 GHz frequency for the Schottky diode has to be determined. The simulated result of S_{21} for 5.2 GHz frequency is shown in Fig. 4.6. The isolation provided by the Schottky Diode is given by

$$Isolation = -20\log(S_{21})dB$$

(4.2)
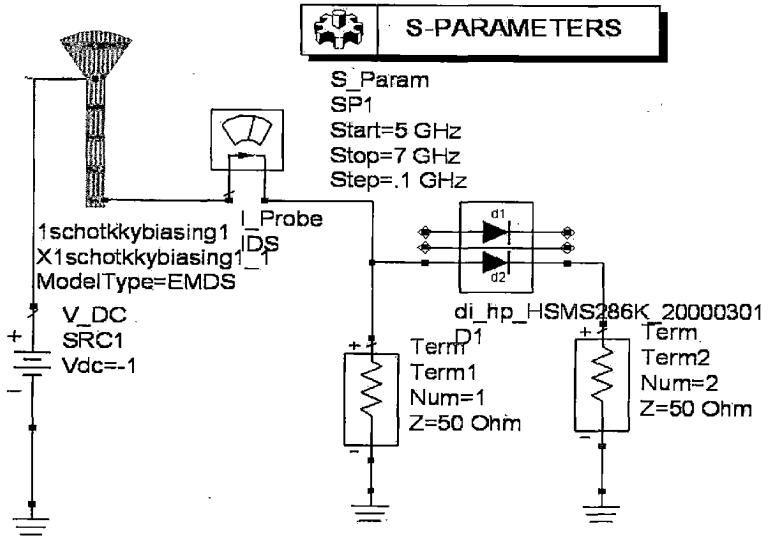
The value of isolation is 15.8 dB for 5.2 GHz frequency.

Fig. 4.5. Circuit setup of the Schottky diode for determining isolation.
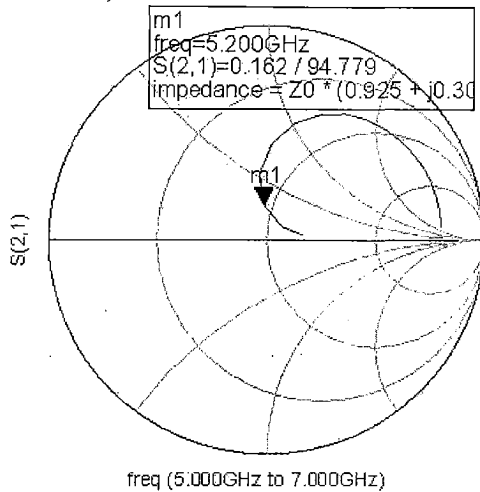

freq (5.000GHz to 7.000GHz)

Fig. 4.6. Resulting forward transmission coefficient for isolation measurement.

4.4   Optimization of Matching circuit

The matching circuit design of both frequencies was discussed in previous chapter. One has to check whether after inducting Schottky diode between the two microstrip resonators, it oscillates at both the frequency or not? This resonator absorbs the diode capacitance into the resonator, thus permit the use of large switches to diminish the Q degradation of the resonator due to the diode switch. Instead of micro-switch, semiconductor switch was used for the selection of frequency band. Schottky diode was used as a band selection switch. At both the frequency negative resistance condition of oscillation will be maintained. Two microstrip resonator using Schottky diode were connected as shown in Fig.4.7. The first microstrip resonator length will be considered for 6.8 GHz and for 5.2 GHz frequency both the microstrip resonator will be considered. OscTest block from ADS have been used to find out whether oscillation will occur when diode is forward or reverse bias.
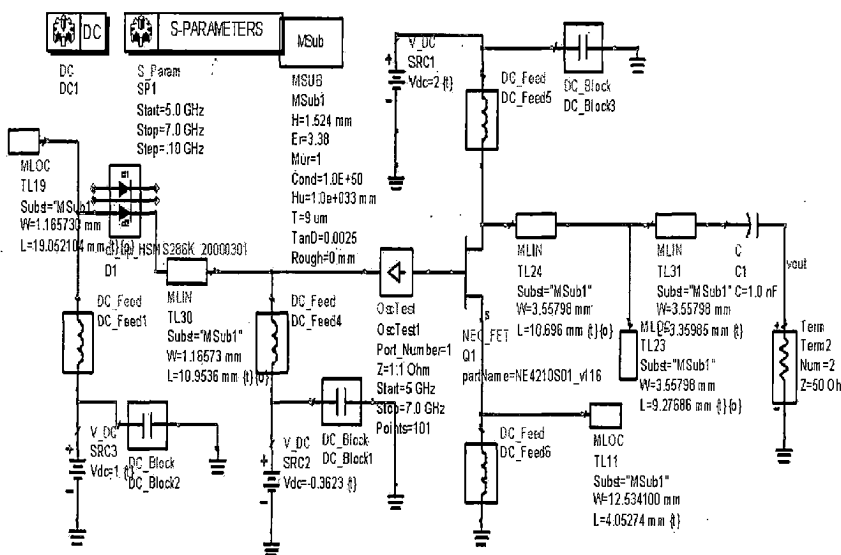

Fig. 4.7. Schematic view of dual band oscillator using Schottky diode.

When Schottky diode is forward bias, it will act as short and the complete length of microstrip line TL19 and TL30 will come in existence with the impedance offered by the diode in forward bias. Hence the complete impedance of TL19, TL30 and impedance offered

by the diode in forward bias with negative resistance will produce oscillation at 5.2 GHz frequency as shown in Fig. 4.8.
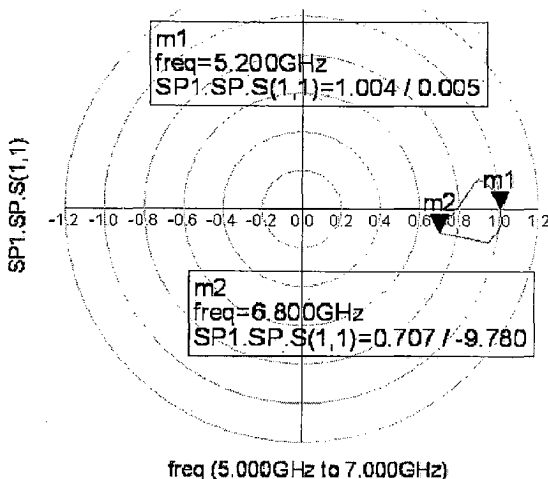

freq (5.000GHz to 7.000GHz)

Fig. 4.8. S-parameter simulation results for forward biased Schottky diode case.
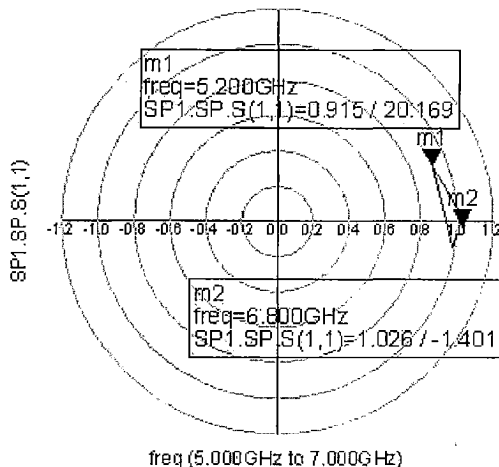

freq (5.000GHz to 7.000GHz)

Fig. 4.9. S-parameter simulation results for reverse biased Schottky diode case.

It has been shown from the simulation results that the magnitude of S_{11} is greater than one and phase is nearly zero at 5.2 GHz frequency in Schottky diode forward bias and the magnitude of S_{11} is less than one at 6.8 GHz frequency. It indicates clearly that the oscillation will occur at 5.2 GHz when Schottky diode is forward biased. When Schottky diode is reverse bias it will act as open circuit and the length of microstrip line TL30 will come in existence with the impedance offered by the diode in reversed bias. Hence the complete impedance of TL30 and impedance offered by the diode in reverse bias with negative resistance will produce oscillation at 6.8 GHz frequency as shown in Fig. 4.9.

In simulation results, it is shown that the magnitude of S_{11} is greater than one at 6.8 GHz frequency in Schottky diode reversed bias and the magnitude of S_{11} is less than one at 5.2 GHz frequency. It clearly indicates that the oscillation occurs at 6.8 GHz when Schottky diode is reverse bias. The next step of the design is to replace lumped elements with microstrip lines. The ADS model was updated to use 'ideal' microstrip lines and open-circuit stubs as shown in Fig. 4.10. The dimensions of the matching network were optimized to get the required frequency of oscillations for both the frequencies. Two different resonators for both the frequencies with insertion of Schottky diode with its biasing circuit were used.
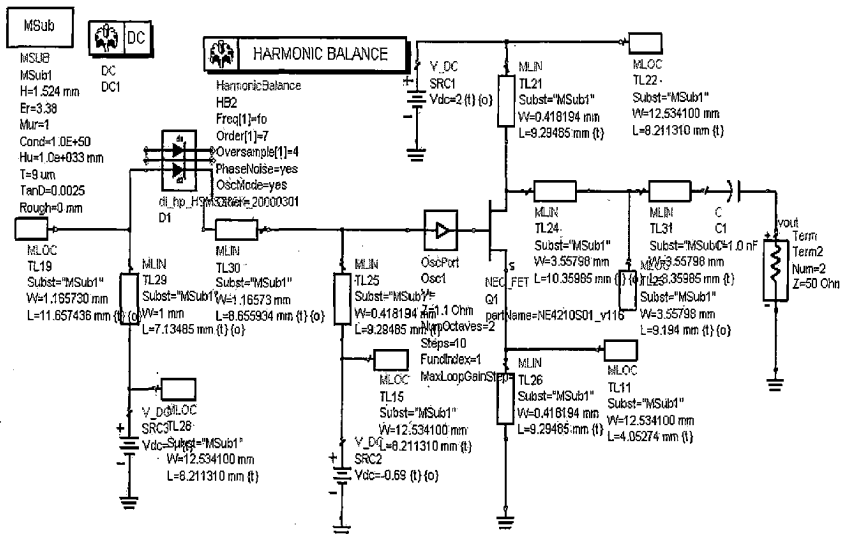
Fig.4.10. Nonlinear analysis of microstrip lines based modified dual band oscillator

In the ADS schematic of the oscillator, A TEE junction was used to connect the three components. The matching network is matched at both the frequencies to a 50Ω line and this 50Ω line does not affect the performance of the oscillator (i.e. frequency of oscillations, output power). The DC Block is a capacitor of 1 nF used to block the DC at the output of oscillator.

4.5   Harmonic Balance Simulation of Dual Band Oscillator:

Nonlinear analysis using harmonic balance simulation to predict the oscillator characteristics i.e. output power spectrum and phase noise performance for both the frequencies will be discussed. The same values for the harmonic balance simulator box have been set as described in previous chapter. The schematic of the harmonic balance ADS simulation of the dual band oscillator design is shown in Fig. 4.11. Here, the "osc port" box is added at a position separating the output and negative resistance region. This box was used for checking the open loop gain of the oscillator. The nonlinear analysis of dual band oscillator is carried out using circuit simulator. The nonlinear harmonic balance analysis was used to compute the output power and phase noise of the designed oscillator. These results were obtained from harmonic balance analysis of circuit shown in Fig. 4.10 is carried out.
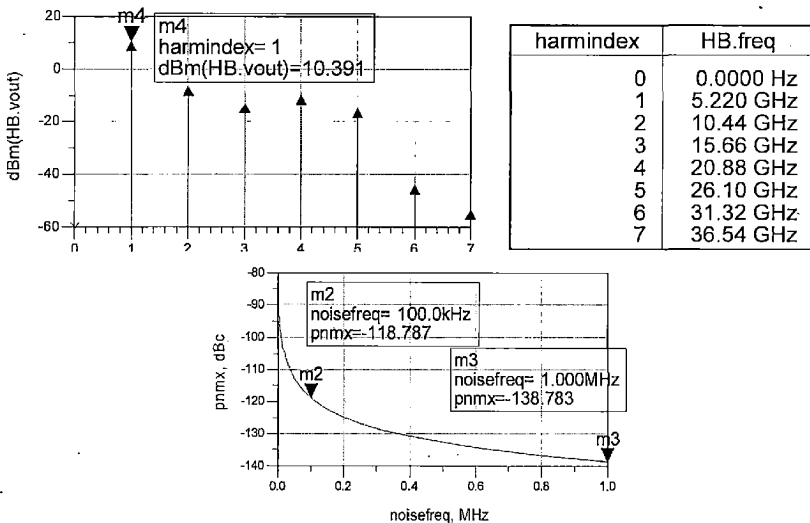

harmindex	HB.freq
0	0.0000 Hz
1	5.220 GHz
2	10.44 GHz
3	15.66 GHz
4	20.88 GHz
5	26.10 GHz
6	31.32 GHz
7	36.54 GHz

Fig. 4.11. Output power and phase noise prediction at 5.2 GHz.

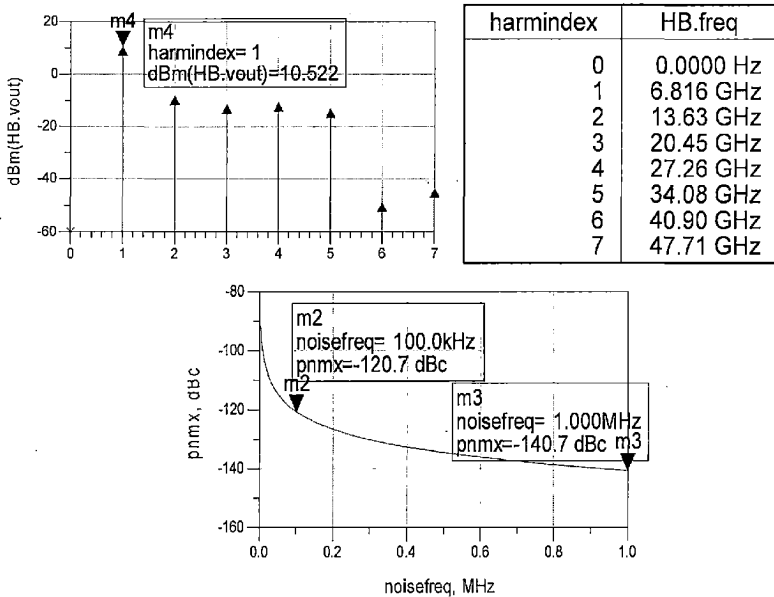| harmindex	HB.freq
0	0.0000 Hz
1	6.816 GHz
2	13.63 GHz
3	20.45 GHz
4	27.26 GHz
5	34.08 GHz
6	40.90 GHz
7	47.71 GHz

Fig. 4.12. Output power and phase noise prediction at 6.8 GHz.

The variation in output power and phase noise of the oscillator at both the frequency is shown in Fig. 4.11 and 4.12. The output power of 10.522 dBm and phase noise of -118.78 dBc/Hz at an offset of 100 KHz from the carrier at the fundamental frequency of 5.2GHz. The output power of 10.522 dBm and phase noise of -120.7 dBc/Hz at an offset of 100 KHz from the carrier at the fundamental frequency of 6.8 GHz.
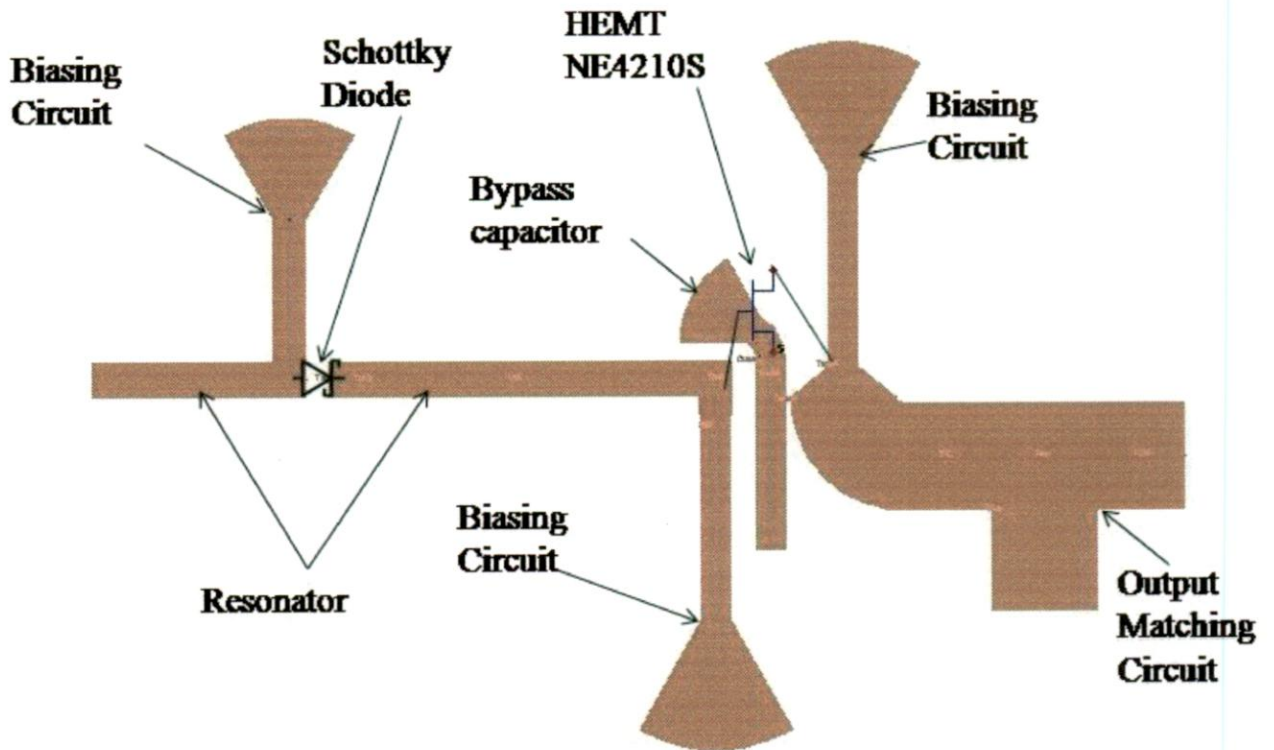
4.6   Full Wave Analysis of Dual Band Oscillator

Finally, the layout without component have been drawn to fine tune dimensions for the final layout using the flow chart for full wave simulation of dual band oscillator using ADS in conjunction with electromagnetic simulation tool momentum. The rectangular microstrip capacitor have been replaced with radial stub. The dimension of radial stub for DC Feed and series feedback resistor after optimization is shown in Table 4.2. for both the frequencies.
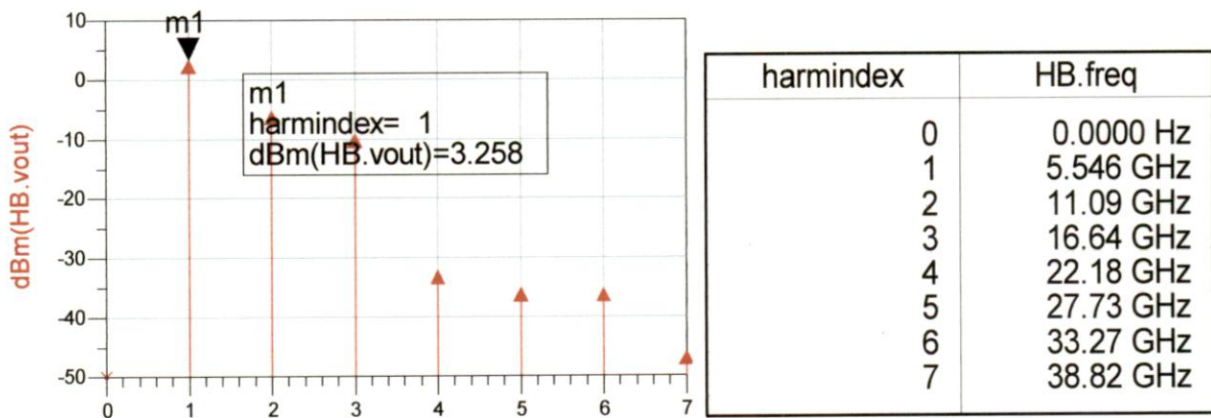
Table 4.2
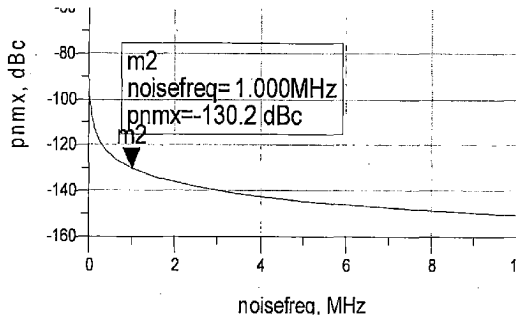**Radial stub dimension for biasing capacitor**

α (degrees)	r_1 (mm)	r_2 (mm)
60	0.418194	4.17713

The simulated layout is shown in Fig. 4.13 and the flow chart for the simulation process was shown in Fig. 3.13. Further optimization was done to get the desired frequency output by manually changing the line lengths and simulations were repeated until a satisfactory output was obtained.
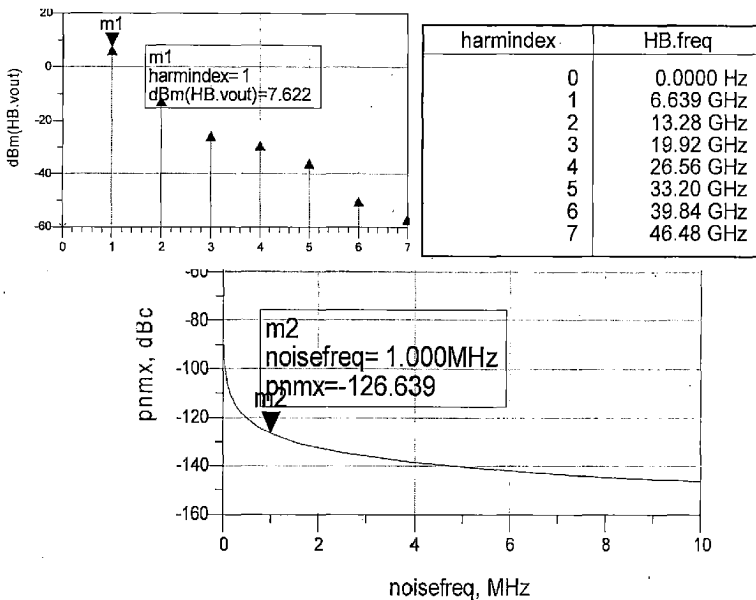

Fig. 4.13 Layout of the designed dual band oscillator using Schottky diode

harmindex	HB.freq
0	0.0000 Hz
1	5.546 GHz
2	11.09 GHz
3	16.64 GHz
4	22.18 GHz
5	27.73 GHz
6	33.27 GHz
7	38.82 GHz

m1
harmindex= 1
dBm(HB.vout)=3.258

Fig. 4.14. Resulting output power and phase noise after full wave simulation at 5.2 GHz

The results obtained after optimization was obtained are shown in Fig. 4.14 and 4.15. The output power has been obtained as 3.258 dBm for 5.2 GHz frequency and 7.62 dBm for 6.8 Ghz frequency, which is 7 dBm less as compared to the result obtained in circuit simulation for 5.2 GHz.

harmindex	HB.freq
0	0.0000 Hz
1	6.639 GHz
2	13.28 GHz
3	19.92 GHz
4	26.56 GHz
5	33.20 GHz
6	39.84 GHz
7	46.48 GHz

Fig. 4.15. Resulting output power and phase noise after full wave simulation at 6.8 GHz

4.7   Characterization of Fabricated Circuits

The optimized circuit was fabricated and the fabrication procedure is explained in Appendix B. The designed circuit was developed and characteristics were measured on spectrum analyzer. The designed layout was fabricated on NH9338 substrate having ϵr =3.38, dielectric thickness of 1.524 mm, copper thickness of 15 to 18 μm and dissipation factor of 0.0025 is shown in Fig. 4.16.
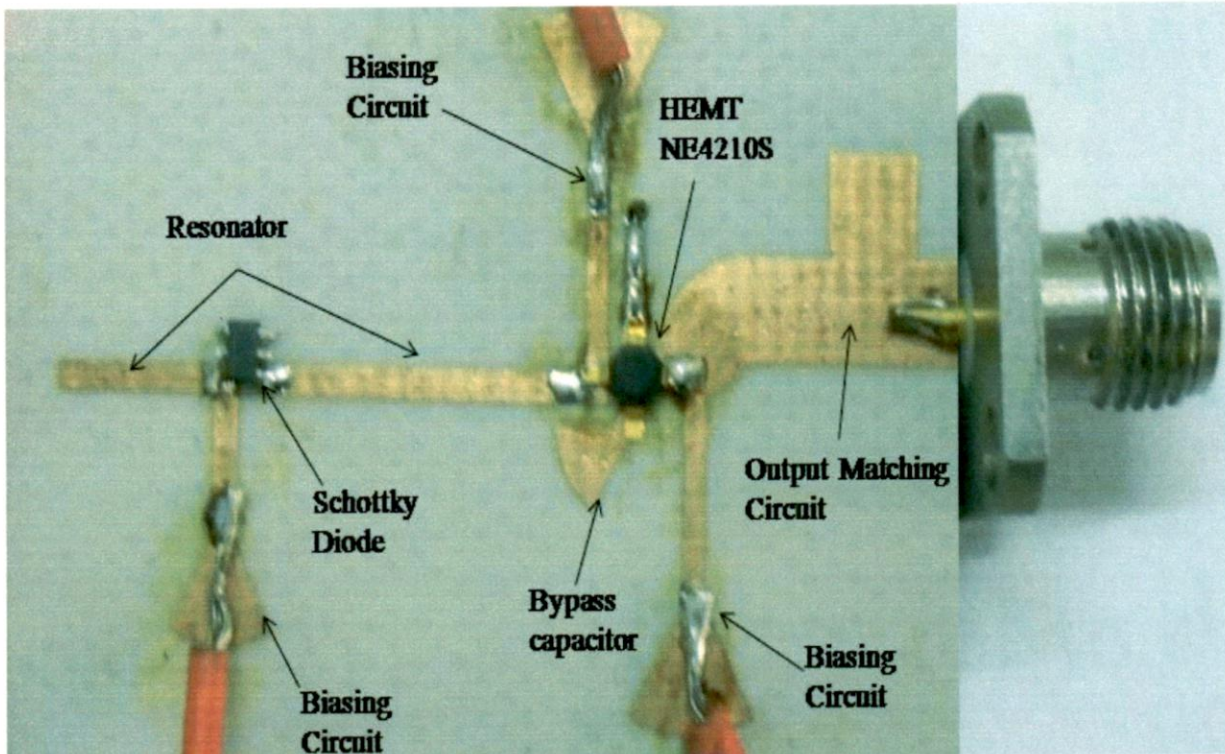

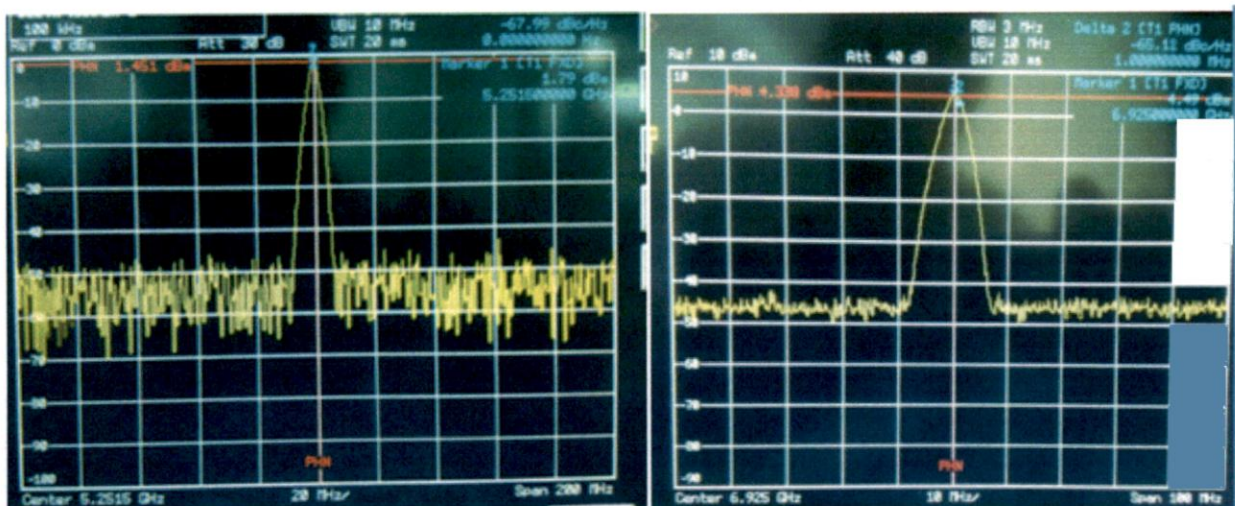Fig. 4. 16. Hardware prototype of dual band oscillator using Schottky diode.

Fig. 4.17 Output power and phase noise on spectrum analyzer at 5.2 and 6.8 GHz

The output power is achieved at desired frequency by varing the biasing voltage along with the supply voltage for the Schottky diode. The measured output power as 1.79 dBm and 4.49 dBm and phase noise has been obtained and -67.99 dBc/Hz and -65.11 dBc/Hz at an offset of 100 KHz for 5.2 GHz and 6.8 GHz respectively as shown in Fig. 4.17. The measured characteristics are generally within 5 –10 % of predictions.

However, the tuning was achieved by varying the biasing voltage. The tuning range of 500 MHz is achieved by varying the biasing voltage of the HEMT in 5.2/6.8 GHz band. The same output power for the biasing voltage Vds=1.7 V and Vgs= -0.4 V has been obtained as 4.02 dBm and phase noise of -116.6 dBc/Hz and -95.03 dBc/Hz at an offset of 1 MHz for 5.7 GHz and 6.48 GHz respectively as shown in Fig. 4.18 and 4.19.
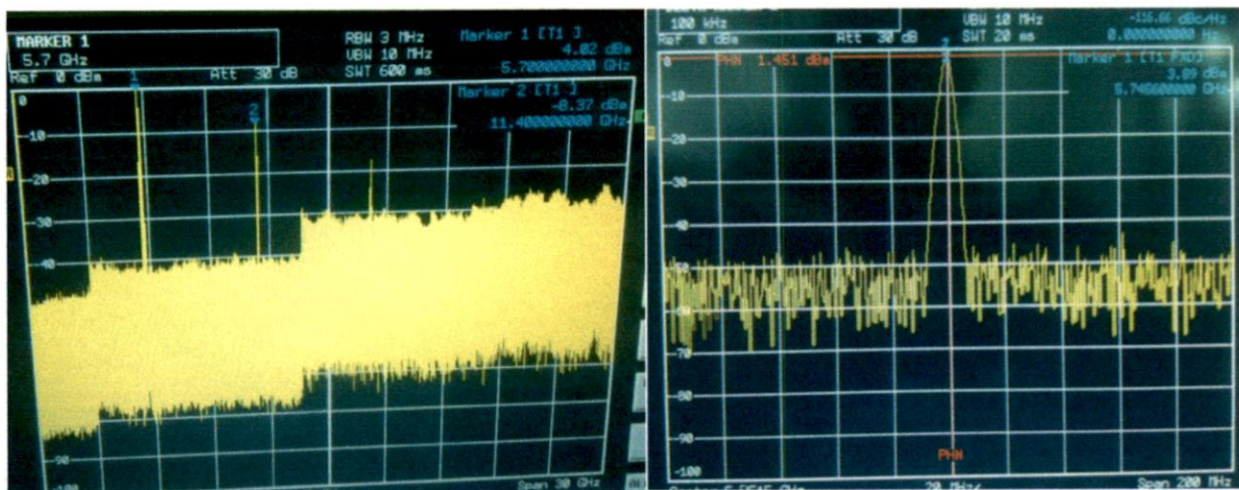
Fig. 4.18 Output power and phase noise on spectrum analyzer at 5.2 GHz
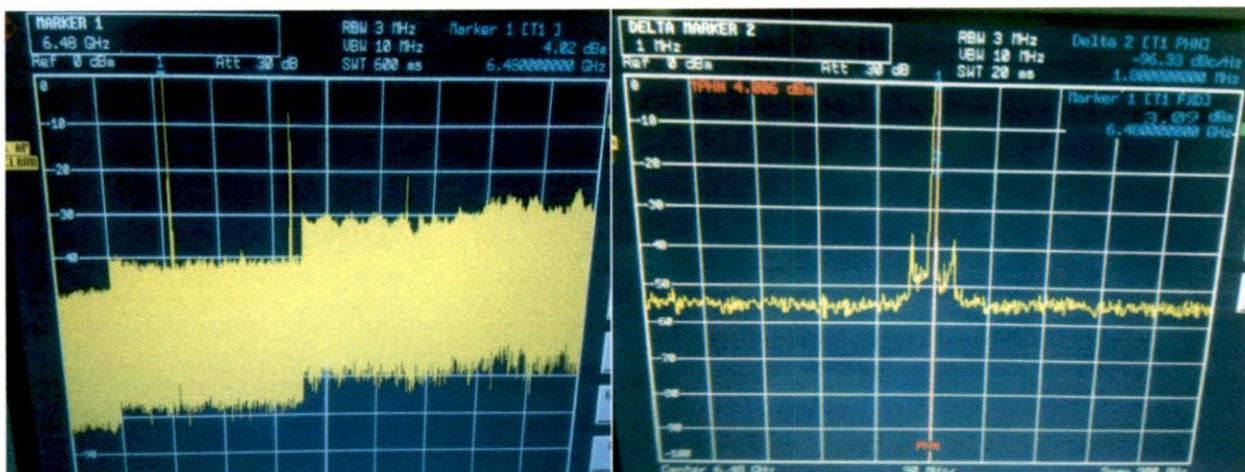
Fig. 4.19 Output power and phase noise on spectrum analyzer at 6.8 GHz

Nonlinear analysis of HEMT based dual band oscillator has been carried out using commercially available circuit simulator alone as well as circuit simulator in combination

with electromagnetic simulator. The numerically obtained output power and phase noise of the fabricated prototype dual band oscillator from both methods are compared and as expected, results obtained from full wave nonlinear analysis differs from circuit simulation because circuit simulator ignores the effect of coupling between lumped and distributed elements. Hence, this full wave nonlinear analysis method can be used to design and accurately predict the behavior of dual band oscillator. The comparison of results obtained from circuit simulation and full wave simulation and fabricated prototype measured from spectrum analyzer is given in Table 4.3.

Table 4.3
Comparison of measured results with the simulated ones

Oscillator Parameter	Circuit Simulation		Full Wave Simulation		Measured on Spectrum Analyzer	
	5.2GHz	6.8GHz	5.2GHz	6.8GHz	5.2GHz	6.8GHz
Output power (dBm)	13.131	14.316	3.258	7.622	1.79	4.49
Phase noise (dBc/Hz at 1 MHz)	-135.34	-131.6	-130.2	-126.6	-96.33	-116.3

4.8   Conclusions

The concept of switched resonator dual band oscillator using semiconductor switchhave been presented. Both Frequency bands (5.2 GHz and 6.8 GHz) are used in commercial wireless applications such as WiMax and WLAN. An excellent agreement was obtained between the theoretical design using full wave nonlinear analysis method and corresponding measured results obtained from fabricated prototype. The tuning of 500 MHz is achieved by varying the biasing voltage. This dual-band oscillator exhibited a phase noise of -67.99 dBc/Hz and -65.11 dBc/Hz at 1 MHz offset and output power of 1.79 dBm and 4.49 dBm operated near 5.2 GHz and 6.8 GHz respectively. This band-switching technique exhibits an outstanding feature of a simplified analog circuitry, miniaturized size, high performance, low cost (single transistor), low supply voltage, low power consumption, high power output.

Integration of Oscillator with Radiating Elements

5.1 *Introduction*

A complete monolithic integration using the active-integrated antenna approach can make the system very compact, low cost, and reliable. When an active device is integrated with a microstrip antenna for the purpose of generating a steady state oscillation, it is classified as an oscillator-type active microstrip antenna. The oscillator converts DC power to RF power using the negative resistance characteristics of active devices. The oscillator consists of an active device in conjunction with a microstrip antenna that simultaneously serves both as a load determining the frequency of oscillation and as an element radiating the generated RF power into space. Proper selection of an operating point of the active device is important for the operational performance. The passive antenna elements and active circuitry are integrated on the same substrate. In this chapter we will development of integrated oscillator with radiating elements at 5.2 GHz fixed frequency, having microstrip patch antenna acting as frequency selective element will be discussed.

5.2 *Basics of Microstrip Patch Antennas:*

The microstrip patch antenna (MPA) is by far the most widely used configuration, consists of radiating patch on one side of the substrate which has ground plane on the other side (refer Fig. 5.1). The patch can take any possible shape. In the present discussion only the rectangular shape of the patch has been used, however various other shapes like triangular, circular, and elliptical or practically any shape can be used. Common shapes are often used, to simplify the analysis and performance prediction. The most common feeding method used for the MPAs is the microstrip line. Other important methods have been mentioned in [33].

Primarily, microstrip patch antennas radiate due to the fringing fields between the patch edge and the ground plane. For a good antenna performance, a thick dielectric substrate having a low dielectric constant is desirable, since this provides better efficiency, larger bandwidth and better radiation. However, such a configuration leads to a larger antenna size. In order to design a compact microstrip patch antenna, higher dielectric constants must be used which are less efficient and result in narrower bandwidth. Hence, a compromise must be reached between antenna dimensions and antenna performance.
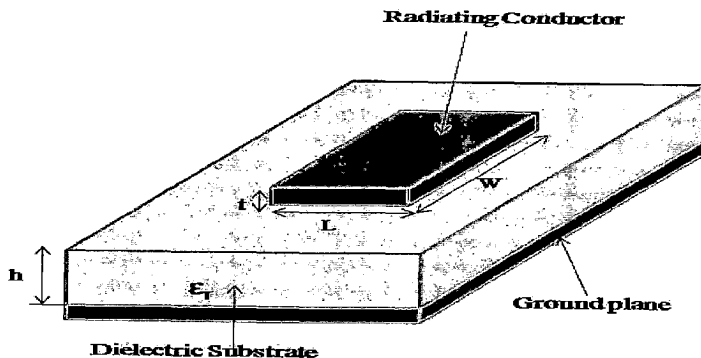
Fig. 5.1. Microstrip Patch Antenna structure

One of the simplest methods of analysis of a microstrip antenna is transmission line method. In Fig. 5.2, most of the electric field lines reside in the substrate and parts of some lines reside in air. An effective dielectric constant (ε_{reff}) must be obtained in order to account for the fringing and the wave propagation in the line. The value of ε_{reff} is slightly less than ε_r because the fringing fields around the periphery of the patch are not confined in the dielectric substrate but are also spread in the air as shown in Fig. 5.2.
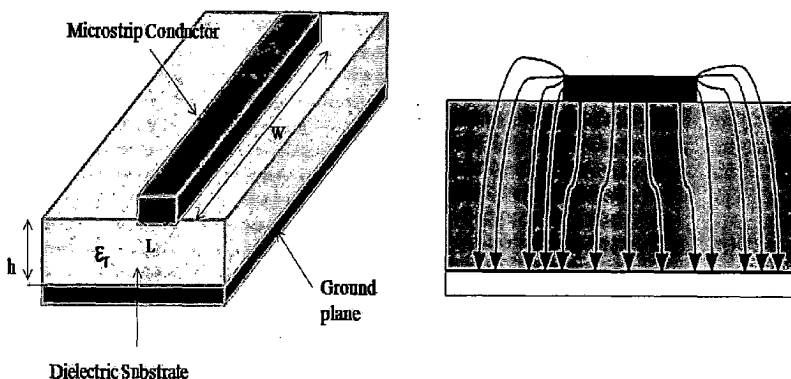

Fig. 5.2. Microstrip line and their electric field distribution

The expression for ε_{reff} is given as [33]:

$$\varepsilon_{reff} = \frac{\varepsilon_r + 1}{2} + \frac{\varepsilon_r - 1}{2}\left[1 + 12\frac{h}{W}\right]^{-\frac{1}{2}} \tag{5.1}$$

Some other relations useful while designing the antenna, given by transmission-line model, are given below. Details of these relations and other relations given by the transmission line model are given in [33]:-

$$\Delta L = 0.412h\frac{\left(\varepsilon_{reff} + 0.3\right)\left(\frac{W}{h} + 0.264\right)}{\left(\varepsilon_{reff} - 0.258\right)\left(\frac{W}{h} + 0.8\right)} \tag{5.2}$$

$$L_{reff} = L + 2\Delta L \tag{5.3}$$

$$L_{reff} = \frac{c}{2f_o\sqrt{\varepsilon_{reff}}} \tag{5.4}$$

$$W = \frac{c}{2f_o\sqrt{\left(\frac{\varepsilon_r + 1}{2}\right)}} \tag{5.5}$$

5.3   *General Design Procedure for a Microstrip Patch Antenna*

First of all, the design of 5.2 GHz patch antenna will be discussed. A patch antenna will be considered as output terminal element for the unstable active device. The coupling effects between the antenna and the RF circuit were ignored at initial stage, but during the non linear analysis these effects will be taken in account. The output power at the input of the antenna is optimized with respect to the constraints imposed by the phase noise and the harmonic levels. Usually, with such a design process, the feeding line loss would be considered negligible. GUI based matlab program (Appendix A) using theory discussed in section 5.2 to find out the physical dimensions of the antenna have been used [39]. One has to feed frequency, dielectric constant and height of dielectric constant as input in the window and output will be antenna parameters W, L, ε_r and input impedance as output as shown in Fig. 5.3. There are two methods of providing feed to the antenna:

1.   Move inside the patch and stop where it provides desired impedance.

2.   Insert a quarter wave transformer between patch and impedance looking from input side of HEMT i.e. 66 Ω for matching the impedance to 66 Ω.
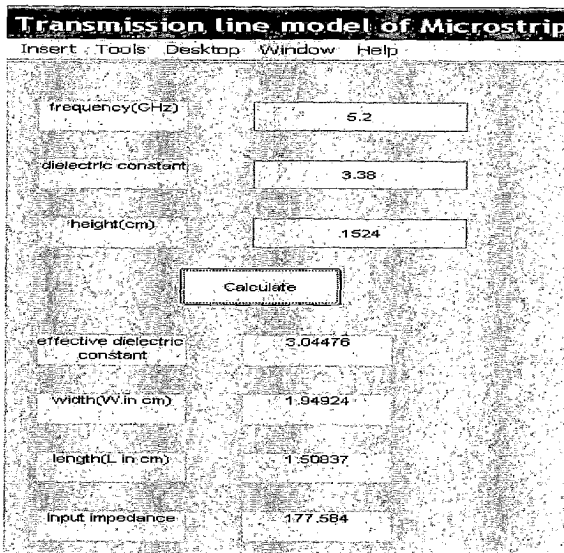
Fig. 5.3. Derived antenna characteristics for 5.2

Second approach was adopted in the present design. The antenna will be taking feed from 66 Ω microstrip line so that oscillator output designed in previous chapters could directly be integrated. For this we add a quarter wave transformer between antenna and oscillator to match antenna impedance with 66 Ω microstrip line. The impedance of this line is given by

$$Z = \sqrt{Z_o Z_{antenna}} = 108\ \Omega \qquad (5.1)$$

Linecal facility was used for calculation of antenna dimensions. The dimensions of the quarterwave transformer is shown in table 5.1.

Table 5.1
Microstrip Line dimensions quarterwave transformer

Z_0 (Ohms)	W (mm)	L (mm)
108 (for 5.2 GHz)	0.720758	9.192790

Now, measure the antenna characteristic by inserting the quarter wave transformer as a feed to the microstrip antenna. One can find that the impedance at measuring port is 66 Ω as

the real part of the impedance looking from the input side of the transformer is 66 Ω. The dimensions of the patch were taken from the Fig. 5.3 for 5.2 GHz frequency. The antenna was considered with a single-port input as shown in Fig. 5.4. (two or more input ports may also be considered) and all the results associated with it, over the frequency band of interest, were transferred to the RF circuit simulator.
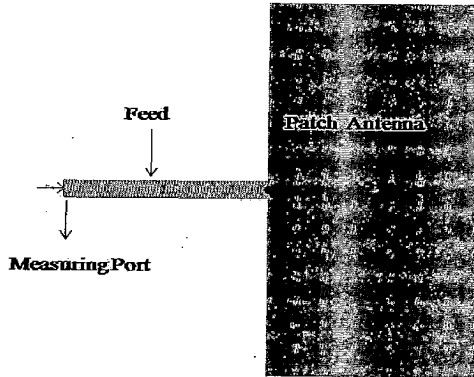

Fig. 5.4. Layout of the designed antenna

The design was carried out firstly by linear simulation to predict the required characteristics. Following this, nonlinear simulation was done to predict the characteristics. Further optimization approach was followed to get the desired frequency by manually change in line lengths and simulations were repeated until a satisfactory output was obtained. The characteristics of the antenna were obtained using the ADS momentum as shown in Fig. 5.5.
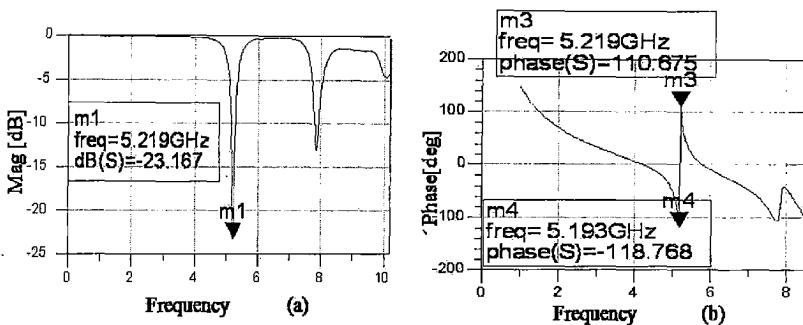

Fig. 5.5. Resulting Antenna characteristics at 5.2 GHz: (a) Magnitude (b) Phase

The optimize dimensions for 5.2 GHz antenna is 19.49x14.5mm for patch and .8x9mm for feed line.. The reflection coefficient or S_{11} for 5.2 GHz -23.167 dBm. The phase crosses zero at desired frequency. That simulation result illustrate that this antenna will radiate at the designed frequency. We will use the physical dimension of antenna directly for 5.2 GHz in next section.

5.4   *Microstrip Patch Antenna as Frequency Selective Network*

Consider a simple design for antenna integrated planar oscillator with convenient controlling of operating frequency. The oscillator design consists of a stable negative resistance circuit and a patch antenna as a resonant element as well as a radiation element. The main advantage is to easily obtain the same oscillation frequency as the antenna radiation frequency. Hence, the antenna radiation frequency automatically becomes oscillation frequency, because antenna acts as frequency selective element.

The design of an oscillator for 5.2 GHz was discussed in Chapter 3. These resonator will be replaced by the radiating element as shown in previous section. However, the coupling effects between the antenna and the other RF circuit elements (matching elements and the DC feeder lines) were ignored. The radiation effects of the antenna feed line were introduced on the antenna side and the input impedance variations of the antenna at the feed line were taken as input parameters for the design of the oscillator. Voltage series feedback was employed to maximize the dynamic range of the oscillator output and to insure that operation fell in the unstable region, as is required to satisfy the oscillation conditions.

Oscillator start-up condition for input port is satisfied i.e. $\Gamma_{in}\Gamma_L= 1$. It verifies that the oscillation frequency is controlled by the size of patch antenna with the negative-resistance circuit. The higher Q factor of patch antenna and slower phase change of active circuit give an oscillation frequency near the antenna radiation frequency. To measure the output power with considering the radiation loss, the patch antennas with the same radiation frequency as the proposed oscillator is used as a reference. The final layout of integrated oscillator with radiating elements for full wave analysis is shown in Fig.5.6. The design was carried out firstly by linear simulation to predict the required characteristics and then nonlinear simulation was carried out to predict the required characteristics.
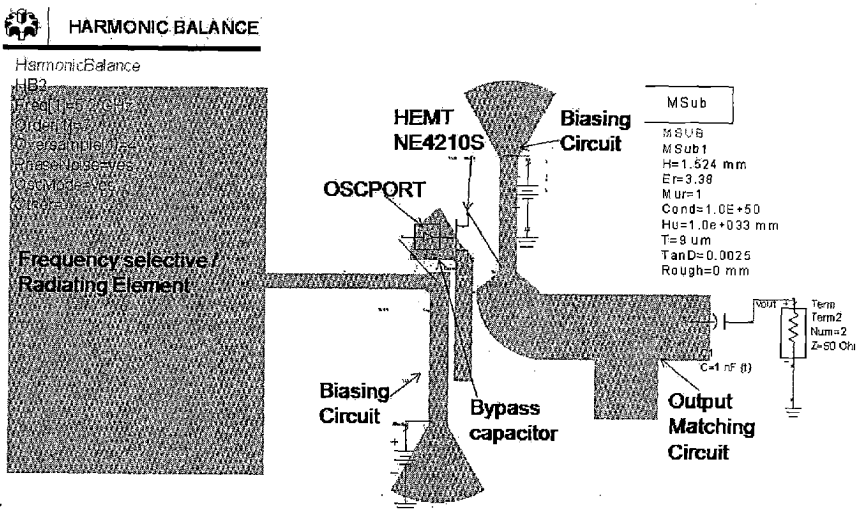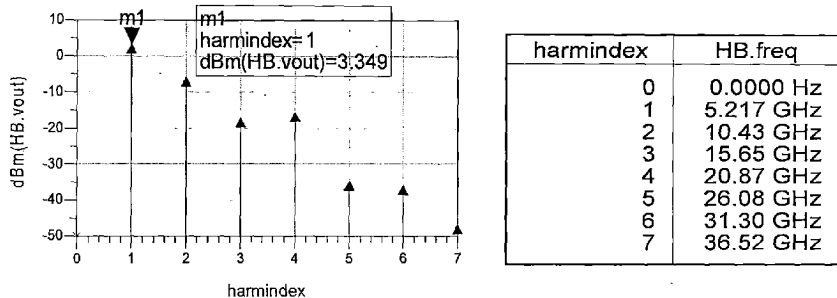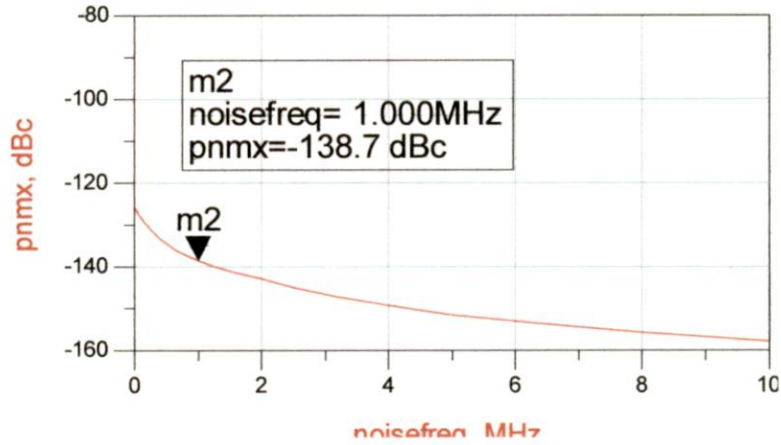
Fig. 5.6. Layout of integrated oscillator with radiating elements at 5.2 GHz.

The nonlinear harmonic balance analysis (implemented in Agilent Advanced Design System (ADS) alone and ADS in conjunction with electromagnetic simulation tool EMDS) were used in determination of oscillator. A rigorous full wave analysis of nonlinear dual band oscillator circuit using electromagnetic simulation tool ADS Momentum in conjunction with Circuit Simulator was performed to compute the output power and phase noise of the designed oscillator as shown in Fig. 5.7. The internal port boundary conditions are used in e. m. simulation to include the effect of radiating element, power supply and transistor in the circuit for full wave analysis, which is the most accurate form of analysis of a design.


harmindex	HB.freq
0	0.0000 Hz
1	5.217 GHz
2	10.43 GHz
3	15.65 GHz
4	20.87 GHz
5	26.08 GHz
6	31.30 GHz
7	36.52 GHz

**Fig. 5.7. Resulting output power and phase noise after full wave simulation at 5.2 GHz**

5.5 Fabrication and Measurements

The fabricated prototype for integrated oscillator active microstrip antenna is shown in Fig. 5.8. The fabrication and testing procedure is explained in Appendix B. The characteristics of the developed circuit are measured. The output power of the oscillator will be radiated from the patch and this patch will act as a resonator. The measured oscillator characteristics at 5.2 GHz frequency is shown in Fig. 5.9.
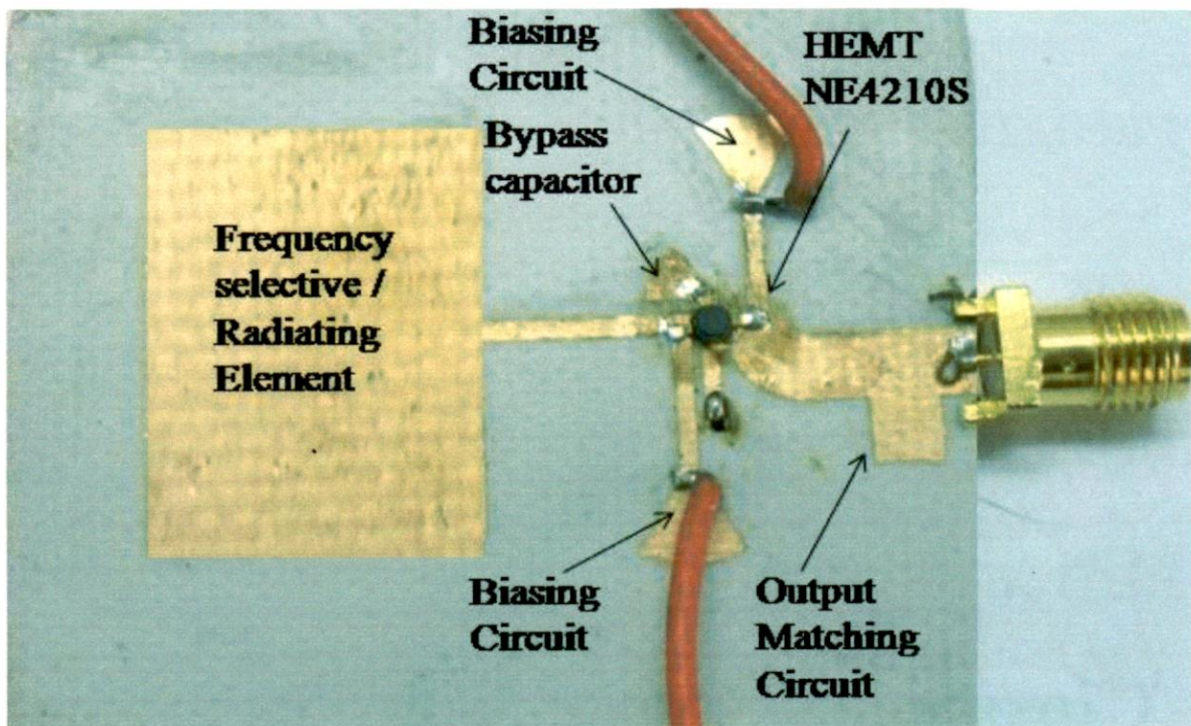
Fig. 5.8. Hardware of integrated oscillator with radiating elements at 5.2 GHz.

The measured output power of 1.33 dBm and phase noise is -67.47 dBc/Hz at an offset of 10 KHz has been obtained for 5.2 GHz frequency. The design goal was met, the measured oscillator phase noise and output power are generally within 2-5 % of predictions.
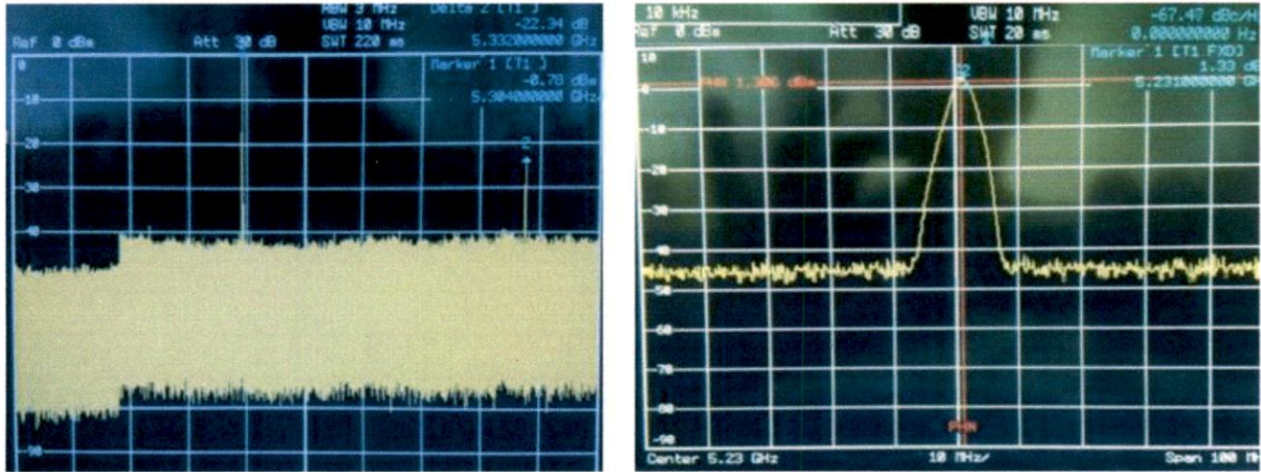
Fig. 5.9. Measured output power and phase noise using spectrum analyzer

5.6 *Conclusions*

The concept of oscillator type active integrated antenna for 5.2 GHz frequency used in commercial wireless applications. An excellent agreement was obtained between the theoretical design using full wave nonlinear analysis method and corresponding measured results obtained from fabricated prototype. This oscillator integrated with radiating elements exhibits a phase noise of -67.47 dBc/ Hz at 10 KHz offset and output power of 1.33. This technique exhibits an outstanding feature of a simplified analog circuitry, miniaturized size, high performance, low cost (single transistor), for low power applications.

Conclusions and Future Scope

6.1 Summary and Conclusion of the Work Done

Rigorous design procedure for dual band oscillator has been presented. Initially, the switched resonator dual band oscillator using membrane switch has been developed. Then the development of dual band oscillator using semiconductor switch was described. Subsequently the concept of AIA was discussed and prototype was developed to justify the concept. First a simple design for microstrip antenna integrated planar oscillator with convenient controlling of operating frequency was demonstrated. Finally the oscillator integration with radiating element is demonstrated. It has been observed that the full wave nonlinear analysis method can be used to design and accurately predict the behavior of dual band oscillator and oscillator with radiating element. These band-switching technique demonstrate an outstanding feature of a simplified analog circuitry, miniaturized size, high performance, low cost (single transistor), low supply voltage, low power consumption, high output power.

6.2 Scope for Further Work

1.   Dual band oscillator canl be converted into a VCO by placing a varactor diode at the gate of the FET which should provide capacitance from 0.1 pF to 1 pF with varying voltage. This will provide tuning of 800 MHz in both the band. Simulation work has already been carried out using a variable capacitor providing capacitance from 0.1 pF to 1 pF.

2.   The designed dual band oscillator can be integrated with dual band antenna with wider bandwidth so that it can be used for its full capability using fractal or slotted or any other method. Designed patch antenna provides low bandwidth.

[1]   A. R. Rofougaran, M. Rofougaran, A. Behzad, "Radios for Next-Generation Wireless Networks," *IEEE Microwave Magazine,* Vol.6, No.1, pp. 38- 43, March 2005.

[2]   Zhenbiao Li , R. Quintal, K. O. Kenneth, "A Dual Band CMOS Front End with two Gain Modes for Wireless LAN Applications," *IEEE Journal of Solid-State Circuits*, Vol. 39, No.11, November 2004.

[3]   J. Ryynanen, S. Lindfors, K. Stadius, K. Halonen, "Integrated Circuits for Multiband Multi mode Receivers," *IEEE Circuits and Systems Magazine*, pp. 5-14, 2006.

[4]   Ulrich L. Rohde, Ajay K. Poddar and Georg Bock, *"The Design of Modern Microwave Oscillators for Wireless Applications,"* John Wiley & Sons, Inc., 2005.

[5]   Guillermo Gonzalez, *"Foundations of Oscillator Circuit Design",* Norwood, MA, Artech House, 2007.

[6]   B. Bakkaloglu, P. Fontaine, "Multi-Mode, Multi-Band RF Transceiver Circuits for Mobile Terminals in Deep-Submicron CMOS Process," *IEEE Radio frequency Integrated Circuits Symposium,* pp.483-486, 2005.

[7]   Sheng Fuh R. Chang, Wen-Lin Chen, Shuen-Chien Chang, Chi-Kang Tu, Chang-Lin Wei, Chen-Hua Tsai, Joe Chen and Albert Chen, "A Dual-Band Transceiver for Multistandard WLAN Applications," *IEEE Transactions on Microwave Theory and Techniques*, Vol. 53, No. 3, March 2005.

[8]   M. Hotti, J. Kaukovuori, J. Ryynanen, J. Kivekas, K. Halonen, "A Direct Conversion RF Front-End for 2 GHz WCDMA and 5.8 GHz WLAN applications," *IEEE Radio Frequency Integrated Circuits Symposium*, pp. 45-48, 2003.

[9]   Cristian Pavao Moreira, Eric Kerherve, Pierre Jarry and Didier Belot, "Design and Implementation of a Dual- Band Concurrent Fully Integrated LNA WLAN IEEE 802.11a/b/g Applications," *Wiley International Journal for RF and Microwave*, 2008.

[10]   David M Pozar, *"Microwave and RF Design of Wireless Systems,"* John Wiley & Sons, 2001.

[11]   Y. Itoh, H. Hasegawa, M. Shirata, and K. Sakamoto, "Supply Voltage Switching Dual-Band SiGe HBT VCOs using a Dual- Band Resonator with Inductor-Loaded Varactor Diode," *IEEE International Microwave Symposium*, pp. 1289-1292, 2009.

[12]   B. U. Klepser, M. Punzenberger, T. Ruhlicke, M. Zannoth, "5-GHz and 2.4-GHz Dual-Band RF-Transceiver for WLAN 802.11a/b/g Applications," *IEEE Radio Frequency Integrated Circuits (RFIC) Symposium*, pp. 37- 40, June 2003.

[13]   Z. Li and K. O. Kenneth, "A 900-MHz 1.5-V CMOS Voltage-Controlled Oscillator using Switched Resonators with a Wide Tuning Range," *IEEE Microwave and Wireless Component Letters*, Vol. 13, No. 4, pp. 137-139, 2003.

[14]   L. Jia, J. G. Ma, K. S. Yeo, X. P. Yu, M. A. Do and W. M. Lim, "A 1.8-V 2.4/5.15-GHz Dual-Band LC VCO in 0.18-μm CMOS Technology," *IEEE Microwave and Wireless Components Letters*, Vol. 16, No. 4, pp. 194-196, April 2006.

[15]   A. Yamagishi, T. Tsukahara, M. Harada, J. Kodate, "A Low-Voltage 6-GHz Band CMOS Monolithic LC-Tank VCO using a Tuning-Range Switching Technique," *IEEE International Microwave Symposium Digest*, Vol. 2, pp.735-738, 2000.

[16]   R. Mukhopadhyay, Chang-Ho Lee, J. Laskar, "A 580-μW 1.8–6 GHz Multiband Switched-Resonator SiGe VCO with 0.3-V Supply Voltage," *IEEE Microwave and Wireless Components Letters*, Vol. 17, No. 11, pp. 793-795, November 2007.

[17]   D. Baek, J. Kim, and S. Hong, "A Dual-Band (13/22-GHz) VCO Based on Resonant Mode Switching," *IEEE Microwave and Wireless Component Letters*, Vol. 13, No. 10, pp. 443-445, Oct. 2003.

[18]   S.-M. Yim and K. O. Kenneth, "Switched Resonators and their Applications in a Dual-Band Monolithic CMOS LC-tuned VCO," *IEEE Transactions on Microwave Theory and Techniques*, Vol. 54, No. 1, pp. 74-81, Jan. 2006.

[19]   Z. Li and K. O. Kenneth, "A Low-Phase-Noise and Low-Power Multiband CMOS Voltage-Controlled Oscillator," *IEEE Journal of Solid State Circuits*, Vol. 40, No. 6, pp. 1296-1302, June 2005.

[20]   P. Andreani,"A 1.8-GHz Monolithic CMOS VCO Tuned by an Inductive Varactor," *IEEE International Symposium on Circuits and Systems*, Vol.4, No., pp.714-717, May 2001.

[21]   B. Catli and M. M. Hella, "A Low-Power Dual-Band Oscillator Based on Band-Limited Negative Resistance," *IEEE International Microwave Symposium Digest*, pp. 251-254, 2009.

[22]   H. C. Shin, Z. Xu, and M. F. Chang, "A 1.8-V 6/9-GHz Switchable Dual-Band Quadrature LC VCO in SiGe BiCMOS Technology," *IEEE Radio Frequency Integrated Circuits (RFIC) Symposium*, pp. 71–74, 2002.

[23]   J. Lin and T. Ttoh, "Active-Integrated Antennas," *IEEE Transactions on Microwave Theory and Techniques*, Vol. 42, pp. 2186-2194, Dec. 1994.

[24]   Kenneth H. Y. Ip, George V. Eleftheriades, "A Compact CPW-based Single-Layer Injection-Locked Active Antenna for Array Applications," *IEEE Transactions on Microwave Theory and Techniques*, Vol. 50, No. 2, pp. 481- 486, February 2002.

[25]   B. Davor and B. Juraj, "Design Considerations of an Active Integrated Antenna with Negative Resistor Transistor Oscillator," *Radioengineering*, Vol. 14, No. 4, pp. 33-39, December 2005.

[26]   X. D. Wu and K. Chang, "Novel Active FET Circular Patch Antenna Arrays for Quasioptical Power Combining", *IEEE Transactions on Microwave Theory and Techniques*, Vol. 42, pp. 766- 771, May 1994.

References

[27] K. Chang, R. A. York, P. S. Hall, and T. Itoh, "Active Integrated Antennas," *IEEE Transactions on Microwave Theory and Techniques*, Vol. 50, pp. 937-944, March 2002.

[28] I. Bahl and P. Bhartia, *"Microwave Solid State Circuit Design,"* John Wiley & Sons, 1988.

[29] A. Hajimiri and T. Lee, "A General Theory of Phase Noise in Electrical Oscillators," *IEEE Journal of Solid-State Circuits*, Vol. 33, pp. 179–194, Feb. 1998.

[30] D. B. Leeson, "A Simple Model of Feedback Oscillator Noise Spectrum," *Proceedings of the IEEE*, Vol. 54, pp. 329–330, 1966.

[31] V. Rizzoli, A. Neri, A. Costanzo, F. Mastri, "Modern Harmonic-Balance Techniques for Oscillator Analysis and Optimization," in *RF and Microwave Oscillator Design*, ed. M. Odyniec, Artech House, 2002.

[32] T. Lee, A. Hajimiri, "Linearity, Time Variation, and Oscillator Phase Noise," in *RF and Microwave Oscillator Design*, ed. M. Odyniec, Artech House, 2002.

[33] C.A Balanis, *"Antenna Theory Analysis and Design,"* John Wiley & Sons, 1997.

[34] G. D. Vendelin, A. M. Pavio, U. L. Rohde, *"Microwave Circuit Design Using Linear and Non Linear Techniques,"* John Wiley & Sons, 1990.

[35] Data Sheet: *"NE 4210S01, Super Low Noise HJ FET,"* California Eastern Laboratory, Santa Clara, CA.

[36] User Manual, Agilent Advanced Design System (2008), Agilent technologies, Palo Alto, CA.

[37] Nagendra Prasad Pathak, Ananjan Basu and Shiban K. Koul, "Full Wave Nonlinear Analysis of Non Radiative Dielectric Guide Circuits including Lumped Elements", *IEEE Transactions on Microwave Theory and Techniques*, Vol. 54, No. 1, pp. 173-179, January 2006

[38] Datasheet: *"HSMS-286x Series, Surface Mount Microwave Schottky Detector Diodes,"* Avago Technologies.

[39] MATLAB 7.2.0.232 (R2006a), The Mathworks Inc.

[1] Ravinder Yadav and N. P. Pathak, "Design and Devlopment of HEMT based Oscillator for Wireless Application," *IEEE-MTTs Student Branch Chapter, IET Alwar* , December 2009.

[2] Ravinder Yadav and N. P. Pathak, "HEMT based Switched Resonator Dual-band Oscillator for Wireless Application," Submitted to *International Conference on Communications, Computers and Devices* (ICCCD) to be held at IIT Kharagpur, Dec. 2010 (review results awaited).

[3] Ravinder Yadav and N. P. Pathak, "Design and Analysis of Switched Resonator Dual Band Oscillator for Wireless Applications," *Microwave and Optical Technology Letters*, June 2010 (Communicated).

Honours Awarded

Received 3rd price by the President, IEEE-MTT-S, for the poster-cum-project presentation [1].

MATLAB Code for Design of Antenna

FUNCTION MICROSTRIP_GUI

% Create and then hide the GUI as it is being constructed.

```
f = figure('Visible','off','Position',[360,380,550,550]);
```

% --- Construct the components.

% --- Construct all textboxes to display variable names.

```
htext1 = uicontrol('Style','text','String','frequency(GHz)',...
'Position',[125,480,90,30]);
htext2 = uicontrol('Style','text','String','dielectric constant',...
'Position',[125,420,90,30]);
htext3 = uicontrol('Style','text','String','height(cm)',...
'Position',[125,360,90,30]);
htext4 = uicontrol('Style','text','String','effective dielectric constant',...
'Position',[125,240,90,30]);
htext5 = uicontrol('Style','text','String','width(W in cm)',...
'Position',[125,180,90,30]);
htext6 = uicontrol('Style','text','String','length(L in cm)',...
'Position',[125,120,90,30]);
htext7 = uicontrol('Style','text','String','input impedance',...
'Position',[125,60,90,30]);
```

% --- Construct textboxes to display output.

```
htext8 = uicontrol('Style','text','String','',...
'Position',[250,240,90,30]);
htext9 = uicontrol('Style','text','String','',...
'Position',[250,180,90,30]);
htext10 = uicontrol('Style','text','String','',...
'Position',[250,120,90,30]);
htext11 = uicontrol('Style','text','String','',...
```

'Position',[250,60,90,30]);

% --- Construct pushbutton.

    hpush = uicontrol('Style','pushbutton','String','Calculate',...

    'Position',[210,300,100,40],...

    'Callback',{@pushbutton1_Callback,htext8,htext9,htext10,htext11});

% --- Construct editboxes to input value from user.

    eth1 = uicontrol('Style','edit',...

    'String','',...

    'Position',[255 480 130 30],...

    'Callback',@edittext1_Callback);

    eth2 = uicontrol('Style','edit',...

    'String','',...

    'Position',[255 420 130 30],...

    'Callback',@edittext2_Callback);

    eth3 = uicontrol('Style','edit',...

    'String','',...

    'Position',[255 360 130 30],...

    'Callback',@edittext3_Callback);

    set([f,hpush,htext1,htext2,htext3,htext4,htext5,htext6,htext7,htext8,htext9,htext10,the

    xt11],...   'Units','normalized')

% Assign the GUI a name to appear in the window title.

    set(f,'Name','Transmission line model of Microstrip Antenna');

 % Move the GUI to the center of the screen.

    movegui(f,'center');

% Make the GUI visible.

    set(f,'Visible','on');

% --- Executes just before untitled is made visible.

    function microstrip_OpeningFcn(hObject, eventdata, handles, varargin)

% h Object   handle to figure

% event data reserved - to be defined in a future version of MATLAB

% handles   structure with handles and user data

% varargin command line arguments to microstrip

% Choose default command line output for microstrip

       handles.output = hObject;

 % Update handles structure

       guidata(hObject, handles);

 % ---- Outputs from this function are returned to the command line.

       function varargout = microstrip_OutputFcn(hObject, eventdata, handles)

% varargout cell array for returning output args

% hObject   handle to figure

% eventdata reserved - to be defined in a future version of MATLAB

% handles   structure with handles and user data

% Get default command line output from handles structure

       varargout{1} = handles.output;

% --- Executes on entering any value in edittext1(frequency)

 function edittext1_Callback(hObject,eventdata,handles)

       global freq;   % --- Declare the variable as global to be used in another function

       freq=0;

       freq = str2double(get(hObject,'String'))

% --- Executes on entering any value in edittext2(dielectric constant(er))

       function edittext2_Callback(hObject,eventdata,handles)

       global er;   % --- Declare the variable as global to be used in another function

       er=0;

       er = str2double(get(hObject,'String'))

% --- Executes on entering any value in edittext3(height)

       function edittext3_Callback(hObject,eventdata,handles)

       global height;   % --- Declare the variable as global to be used in another function

       height=0;

       height = str2double(get(hObject,'String'))

% --- Executes on button press in pushbutton1.

       function pushbutton1_Callback(hObject, eventdata,htext8,htext9,htext10,htext11)

% --- To use a global variable

       global freq;

       global er;

```
        global height;
% --- Calculate various parameters of microstrip antenna using
% transmission line model.
        c=3*10^10;
        Width=(c/(2*freq*10^9))*(sqrt(2/(er+1)))
        ereff=(er+1.0)/2.0+(er-1)/(2.0*sqrt(1.0+12.0*height/Width))
        dl=0.412*height*((ereff+0.3)*(Width/height+0.264))/((ereff-.258)*(Width/height+0.8))
        lamda=30.0/(freq*sqrt(ereff))
        lamda0=30.0/freq
        Leff=lamda/2
        L=Leff-2*dl
        if Width<(lamda0/10)
            G1=Width^2/(90*lamda0^2)
        else
            G1=Width/(120*lamda0)
        end
        Zin= 1/(2*G1)
% --- To display the resultant values in output textboxes.
        set(htext8,'String',ereff);
        set(htext9,'String',Width)
        set(htext10,'String',L)
        set(htext11,'String',Zin)
```

Fabrication & Testing

Fabrication

The oscillator has been fabricated and tested using the spectrum analyzer. The return loss of the antenna was measured with the HP 8720B Network Analyzer. The designed layout was fabricated on NH9338 substrate having ϵr =3.38 and 1.524 mm thickness (15 to 18 µm copper thickness, dissipation factor of 0.0025) using lithography techniques for antenna and oscillator. Lithography is typically the transfer of a layout pattern to a photosensitive material by selective exposure to a radiation source such as light. A photosensitive material is a material that experiences a change in its physical properties when exposed to a radiation source. If we selectively expose a photosensitive material to radiation (e.g. by masking some of the radiation) the pattern of the radiation on the material is transferred to the material exposed. In lithography, the photosensitive material used is typically a photo resist. When resist is exposed to a radiation source of a specific wavelength, the chemical resistance of the resist to developer solution changes. If the resist placed in a developer solution after selective exposure to a light source, it will etch away one of the two regions (exposed or unexposed). If the exposed material is etched away by the developer and the unexposed region is resilient, the material is considered to be a positive resist. If the exposed material is resilient to the developer and the unexposed region is etched away, it is considered to be a negative resist. The photo resist used here was a negative resist.

Testing

After fabrication of the layout was completed, lumped components, supply wires and transistor were added to the matching section by soldering. For oscillator characteristics i.e. phase noise and output power measurements we connect the oscillator to power supply and spectrum analyzer. The start frequency was set to 2 GHz and stop frequency to 9 GHz. For return loss or S_{11} parameter of the antenna was measured with the Network Analyzer. The start frequency was set to 5 GHz and stop frequency to 7.5 GHz. Single port calibration of the network analyzer was done before connecting the antenna. A print out of the measured results was taken which has been shown in this report.

CEL NEC's SUPER LOW NOISE HJ FET | NE4210S01

FEATURES

- **SUPER LOW NOISE FIGURE:**
  0.50 dB TYP at f = 12 GHz
- **HIGH ASSOCIATED GAIN:**
  13.0 dB TYP at f = 12 GHz
- **GATE LENGTH:** LG ≤ 0.20 μm
- **GATE WIDTH:** WG = 160 μm

DESCRIPTION

NEC'S NE4210S01 is a pseudomorphic Hetero-Junction FET that uses the junction between Si-doped AlGaAs and undoped InGaAs to create very high mobility electrons. The device features mushroom shaped TiAl gates for decreased gate resistance and improved power handling. Its excellent low noise figure and high associated gain make it suitable for DBS and commercial systems. The NE4210S01 is housed in a low cost plastic package which is available in tape and reel.

NEC's stringent quality assurance and test procedures assure the highest reliability and performance.

OUTLINE DIMENSION (Units in mm)

PACKAGE OUTLINE SO1
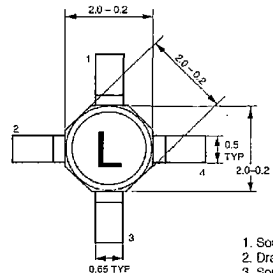
1. Source
2. Drain
3. Source
4. Gate
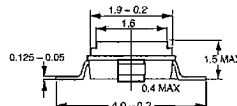
ELECTRICAL CHARACTERISTICS (TA = 25°C)

PART NUMBER PACKAGE OUTLINE			NE4210S01 S01		
SYMBOLS	PARAMETERS AND CONDITIONS	UNITS	MIN	TYP	MAX
GA	Associated Gain[1], VDS = 2 V, ID = 10 mA, f = 12 GHz	dB	11.0	13.0	
NF	Noise Figure[1], VDS = 2 V, ID = 10 mA, f = 12 GHz	dB		0.50	0.70
gm	Transconductance, VDS = 2 V, ID = 10 mA	mS	40	55	
IDSS	Saturated Drain Current, VDS = 2 V, VGS = 0 V	mA	15	40	70
VP	Gate to Source Cutoff Voltage, VDS = 2 V, ID = 100 μA	V	-0.2	-0.7	-2.0
IGSO	Gate to Source Leakage Current, VGS = -3 V	μA		0.5	10

Note:
1. Typical values of noise figures and associated gain are those obtained when 50% of the devices from a large number of lots were individually measured in a circuit with the input individually tuned to obtain the minimum value. Maximum values are criteria established on the production line as a "go-no-go" screening tuned for the "generic" type but not each specimen.

California Eastern Laboratories

CAD Assisted Development of Dual Band Oscillator and its Integration with Radiating elements

NE4210S01

ABSOLUTE MAXIMUM RATINGS[1] (TA = 25°C)

SYMBOLS	PARAMETERS	UNITS	RATINGS
V_{DS}	Drain to Source Voltage	V	4.0
V_{GS}	Gate to Source Voltage	V	-3.0
I_{DS}	Drain Current	mA	I_{DSS}
I_{GS}	Gate Current	µA	100
P_T	Total Power Dissipation	mW	165
T_{CH}	Channel Temperature	°C	125
T_{STG}	Storage Temperature	°C	-65 to +125

Note:
1. Operation in excess of any one of these parameters may result in permanent damage.

TYPICAL MOUNT PAD LAYOUT (Units in mm)
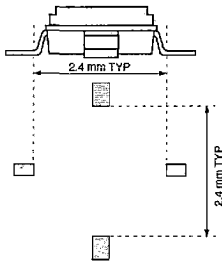
RECOMMENDED OPERATING CONDITIONS (TA = 25°C)

	PART NUMBER		NE4210S01		
SYMBOLS	PARAMETERS	UNITS	MIN	TYP	MAX
V_{DS}	Drain to Source Voltage	V		2	3
I_{DS}	Drain Current	mA		10	15
P_{IN}	Input Power	dBm			0

TYPICAL NOISE PARAMETERS (TA = 25°C)

FREQ.	NFMIN	GA	ГOPT		Rn/50
(GHz)	(dB)	(dB)	MAG	ANG	
V_{DS} = 2 V, I_D = 10 mA					
2.0	0.29	20.7	0.94	12	0.38
4.0	0.30	18.7	0.80	26	0.33
6.0	0.33	17.0	0.66	44	0.26
8.0	0.38	15.4	0.50	68	0.18
10.0	0.43	14.1	0.38	97	0.11
12.0	0.50	13.0	0.29	133	0.09
14.0	0.59	12.3	0.27	177	0.08
16.0	0.71	11.8	0.33	-129	0.11
18.0	0.86	11.2	0.39	-82	0.23

ORDERING INFORMATION

PART NUMBER	SUPPLY FORM	MARKING
NE4210S01	Bulk, min.	
NE4210S01-T1	Tape & Reel 1000 pcs/reel	
NE4210S01-T1B	Tape & Reel 4000 pcs/reel	

Appendix C

TYPICAL PERFORMANCE CURVES (TA = 25°C)

DRAIN CURRENT vs. DRAIN TO SOURCE VOLTAGE

Drain to Source Voltage, VDS (V)

DRAIN CURRENT vs. GATE TO SOURCE VOLTAGE

Gate to Source Voltage, VGS (V)

TOTAL POWER DISSIPATION vs. AMBIENT TEMPERATURE

Ambient Temperature, TA (°C)

MAXIMUM AVAILABLE GAIN, FORWARD INSERTION GAIN vs. FREQUENCY

Frequency, f (GHz)

NOISE FIGURE & ASSOCIATED GAIN vs. FREQUENCY

Frequency, f (GHz)

NOISE FIGURE and ASSOCIATED GAIN vs. DRAIN CURRENT

Drain Current, ID (mA)

CAD Assisted Development of Dual Band Oscillator and its Integration with Radiating elements

[83]

Surface Mount Microwave Schottky Detector Diodes

∴∴ Agilent Technologies
Innovating the HP Way

Technical Data

HSMS-286x Series

Features

- High Detection Sensitivity:
  up to 50 mV/μW at 915 MHz
  up to 35 mV/μW at 2.45 GHz
  up to 25 mV/μW at 5.80 GHz
- Low FIT (Failure in Time) Rate*
- Tape and Reel Options Available
- Unique Configurations in Surface Mount SOT-363 Package
  – increase flexibility
  – save board space
  – reduce cost
- HSMS-286K Grounded Center Leads Provide up to 10 dB Higher Isolation
- Matched Diodes for Consistent Performance
- Better Thermal Conductivity for Higher Power Dissipation

SOT-363 Package Lead Code Identification (top view)

HIGH ISOLATION
UNCONNECTED PAIR
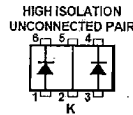
Pin Connections and Package Marking
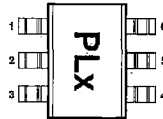
Notes:
1. Package marking provides orientation and identification.
2. The first two characters are the package marking code. The third character is the date code.

Description

Agilent's HSMS-286x family of DC biased detector diodes have been designed and optimized for use from 915 MHz to 5.8 GHz. They are ideal for RF/ID and RF Tag applications as well as large signal detection, modulation, RF to DC conversion or voltage doubling.

Available in various package configurations, this family of detector diodes provides low cost solutions to a wide variety of design problems. Agilent's manufacturing techniques assure that when two or more diodes are mounted into a single surface mount package, they are taken from adjacent sites on the wafer, assuring the highest possible degree of match.

SOT-323/SOT-363 DC Electrical Specifications, T_C = +25°C, Single Diode

Part Number HSMS-	Package Marking Code[1]	Lead Code	Configuration	Forward Voltage V_F (mV)		Typical Capacitance C_T (pF)
286K	TK	K	High Isolation Unconnected Pair	250 Min.	350 Max.	0.25
Test Conditions				I_F = 1.0 mA		V_R = 0 V, f = 1 MHz

Notes:
1. Package marking code is laser marked.

Absolute Maximum Ratings, T_C = +25°C, Single Diode

Symbol	Parameter	Unit	Abs Max[1] SOT-323/363
P_{IV}	Peak Inverse Voltage	V	4.0
T_J	Junction Temperature	°C	150
T_{STG}	Storage Temperature	°C	-65 to 150
T_{OP}	Operating Temperature	°C	-65 to 150
θ_{jc}	Thermal Resistance[2]	°C/W	150

Notes:
1. Operation in excess of any one of these conditions may result in permanent damage to the device.
2. T_C = +25°C, where T_C is defined to be the temperature at the package pins where contact is made to the circuit board.

CAD Assisted Development of Dual Band Oscillator and its Integration with Radiating elements

Equivalent Linear Circuit Model,
Diode chip
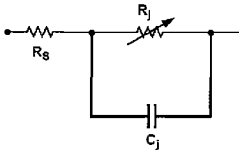
R_S = series resistance (see Table of SPICE parameters)

C_j = junction capacitance (see Table of SPICE parameters)

$$R_j = \frac{8.33 \times 10^{-5} \, nT}{I_b + I_s}$$

where

I_b = externally applied bias current in amps

I_s = saturation current (see table of SPICE parameters)

T = temperature, °K

n = ideality factor (see table of SPICE parameters)

SPICE Parameters

Parameter	Units	Value
B_V	V	7.0
C_{J0}	pF	0.18
E_G	eV	0.69
I_{BV}	A	1 E - 5
I_S	A	5 E - 8
N		1.08
R_S	Ω	6.0
P_B (VJ)	V	0.65
P_T (XTI)		2
M		0.5

Typical Parameters, Single Diode
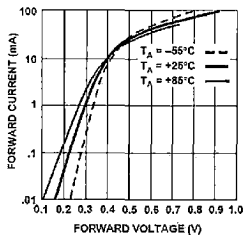
Figure 1. Forward Current vs.
Forward Voltage at Temperature.
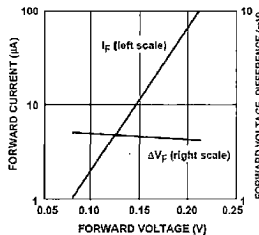
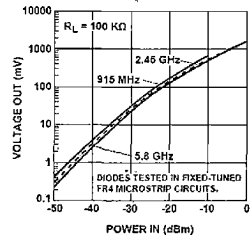Figure 2. Forward Voltage Match.

Figure 3. +25°C Output Voltage vs.
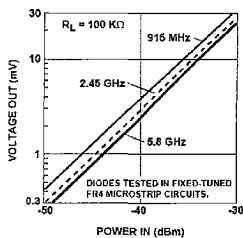Input Power. 3 μA Bias.

Figure 4. +25°C Expanded Output
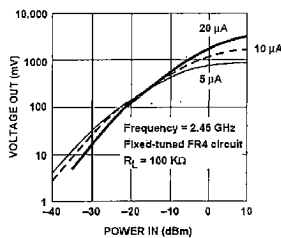Voltage vs. Input Power. See Figure 3.

Figure 5. Dynamic Transfer
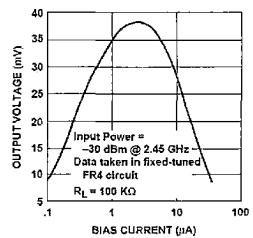Characteristic as a Function of DC Bias.

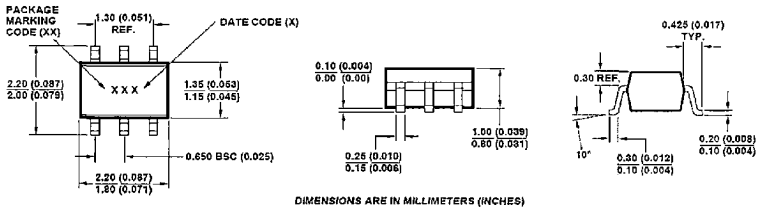Figure 6. Voltage Sensitivity as a
Function of DC Bias Current.

Package Dimensions

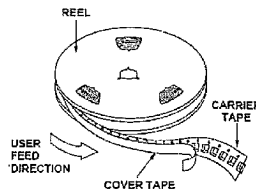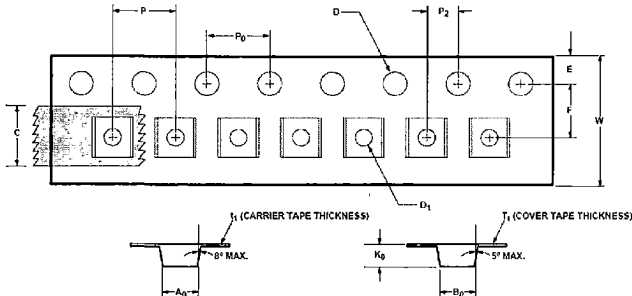### Outline SOT-363
(SC-70, 6 Lead)

DIMENSIONS ARE IN MILLIMETERS (INCHES)

Part Number Ordering Information

Part Number	No. of Devices	Container
HSMS-286x-TR2*	10000	13" Reel
HSMS-286x-TR1*	3000	7" Reel
HSMS-286x-BLK*	100	antistatic bag

where x = 0, 2, 3, 4, 5, B, C, E, F, K, L, P or R for HSMS-286x.

Device Orientation

Tape Dimensions and Product Orientation
For Outline SOT-323 (SC-70 3 Lead)

	DESCRIPTION	SYMBOL	SIZE (mm)	SIZE (INCHES)
CAVITY	LENGTH	A_0	2.24 ± 0.10	0.089 + 0.004
	WIDTH	B_0	2.34 ± 0.10	0.092 ± 0.004
	DEPTH	K_0	1.22 ± 0.10	0.048 ± 0.004
	PITCH	P	4.00 ± 0.10	0.157 ± 0.004
	BOTTOM HOLE DIAMETER	D_1	1.00 + 0.25	0.039 + 0.010
PERFORATION	DIAMETER	D	1.55 ± 0.05	0.061 ± 0.002
	PITCH	P_0	4.00 ± 0.10	0.157 ± 0.004
	POSITION	E	1.75 ± 0.10	0.069 ± 0.004
CARRIER TAPE	WIDTH	W	8.00 ± 0.30	0.315 ± 0.012
	THICKNESS	t_1	0.255 ± 0.013	0.010 ± 0.0005
COVER TAPE	WIDTH	C	5.4 ± 0.10	0.205 ± 0.004
	TAPE THICKNESS	T_1	0.062 ± 0.001	0.0025 ± 0.00004
DISTANCE	CAVITY TO PERFORATION (WIDTH DIRECTION)	F	3.50 ± 0.05	0.138 ± 0.002
	CAVITY TO PERFORATION (LENGTH DIRECTION)	P_2	2.00 ± 0.05	0.079 + 0.002